BEAM-FOIL LIFETIMES OF FeI

by

Michael H. Fox

B.S., McPherson College, 1968

A MASTER'S THESIS

submitted in partial fulfillment of the

requirements for the degree

MASTER OF SCIENCE

Department of Physics

KANSAS STATE UNIVERSITY
Manhattan, Kansas

1972

Approved by:

C. L. Cocke

Major Professor

TABLE OF CONTENTS

INTRODUCTION

Iron has held a long-standing interest for astrophysicists. There are several reasons for this. A graph of elemental abundances in the solar system reveals that there is an abundance peak centered on Fe^{56} (Clayton 1968). The iron group (nuclei in the abundance peak centered on Fe^{56}, primarily Cr, Mn, Fe, Co, and Ni), and iron in particular, are therefore important in testing theories of stellar nucleosynthesis. Because of their large abundances, these elements are important in determining radiative opacities. The importance of iron for the solar opacity is discussed by Watson (1969). Further, the visible solar spectrum is dominated by thousands of neutral iron lines, making iron very useful in studying many properties of the sun.

One of the most important methods of determining stellar abundances relies on the "curve of growth" technique (Motz 1970). A curve of growth is a relation between the equivalent width of a stellar line and the number of absorbing atoms producing it. A stellar model is employed to calculate a theoretical curve of growth for a particular element, which is then compared with an observational curve of growth that depends on the f-value of the line. The abundance of the element can be found from the comparison. Since f-values are related to transition probabilities, it is of great importance in determining elemental abundances to have accurate transition probabilities.

There has been a long-standing discrepancy in the photospheric and coronal abundances of iron (Muller 1966), with the photospheric abundance being lower by a factor of 10 to 20. The curve of growth calculations for the photospheric abundance has relied primarily on the oscillator strengths given in Corliss and Bozman (1962), Corliss and Warner (1964), or Corliss and Tech (1967). Recent determinations of f-values for FeI indicate that these

oscillator strengths are in error by as much as a factor of 20. These f-values are given by Huber and Tobey (1968); Grasdalen, Huber, and Parkinson (1969); Garz and Kock (1969); Whaling, King, and Martinez-Garcia (1969); Bridges and Wiese (1970); Whaling, Martinez-Garcia, Mickey, and Lawrence (1970); Wolnik, Berthel, and Wares (1971); and Huber and Parkinson (1971). The results indicate that the photospheric abundance should be raised by a factor of 5 to 10. They also indicate that there is a normalization error in the compilations of Corliss and co-workers, and furthermore that it depends on the excitation energy of the upper level.

The new transition probabilities have been determined by a variety of methods, including arc emission, shock tube emission, shock tube absorption, and beam-foil spectroscopy. There is a current need for more data, however, since many of the lines in the various experiments do not overlap. Beam-foil spectroscopy offers one of the most direct methods of measuring oscillator strengths or transition probabilities by measuring directly the lifetime of an atomic energy level. It thus avoids the serious problem inherent in arc and shock tube work of knowing accurately the number densities of emitting species. Because of this problem, it is very difficult to obtain accurate absolute transition probabilities, although relative transition probabilities may be quite accurate. Beam-foil spectroscopy is very useful because although it allows an accurate determination of a rather limited number of transition probabilities, these can then be used to fix an absolute scale for the relative transition probabilities.

It will be the purpose of this thesis to describe the method of beam-foil spectroscopy and how it was used to determine the lifetimes of several states in FeI. These lifetimes will be compared with the results of Corliss and Tech, Corliss and Bozman, and other researchers where possible. Of par-

ticular interest is the comparison with the results of Whaling, et. al., (1970), who has also used beam-foil spectroscopy to measure lifetimes of FeI but at higher beam energies.

BEAM-FOIL SPECTROSCOPY

Beam-foil spectroscopy is a relatively new and powerful weapon in the arsenal of atomic physics research for studying energy level structure and transition probabilities. The technique of beam-foil spectroscopy was developed principally by Bashkin in 1964. (See Bashkin, Malmberg, Meinel, and Tilford 1964; Bashkin, Heroux, and Shaw 1964; Bashkin and Meinel 1964. For a general review, see Bashkin 1968 and 1970.)

The general procedure for doing beam-foil experiments is to produce a beam of the particular atom to be studied and accelerate it into a thin foil. During the collisional processes which occur in passing through the foil, the ions may be further ionized or may capture electrons to become neutral atoms, depending on the energies used and the thickness of the foil. A further result of the ion-foil interaction is the excitation of the ions or atoms to many different energy states.

As the beam of particles leaves the foil, the electrons make transitions from the excited levels to lower energy levels, producing a visible beam that diminishes in intensity as a function of distance from the foil. From a wavelength scan of the glowing beam, the spectrum may be analyzed to determine the lines present. The upper and lower levels of the transitions may then be found in Atomic Energy Levels (Moore 1952). The velocity of the beam must be calculated from the post-foil energy or measured directly. From the known beam velocity, the distance from the foil may be calibrated as a time axis. The slope of the decay curve for a particular line allows one to measure the mean lifetime of the upper level directly. From the lifetime, the absolute transition probability may be determined directly if there is only one strong transition. Otherwise, branching ratios of all

the lines from the upper level being studied must be measured to yield the transition probability.

Beam-foil spectroscopy thus provides a rather elegant technique for determining absolute transition probabilities, without requiring a knowledge of population densities of the levels involved or plasma temperatures, both of which are problems for arc and shock tube experiments. Further, by accelerating the incident ion to high energies, highly stripped atoms may be examined without the necessity of the very high temperatures that would be required for an arc source. This makes it of particular use in studying lines from atoms in high charge states, which are prevalent in the solar corona. Therefore, beam-foil spectroscopy has great utility as a tool for providing atomic data of particular use to the astrophysicist.

There are, however, certain inherent problems in the beam-foil method. Doppler broadening of the spectral lines makes line identification difficult in a high line-density region of the spectrum and limits the resolution that may be obtained. Due to the non-selective excitation process, many different levels are populated and cascading from higher levels becomes a very serious problem for levels lying at a low excitation potential. This feeding of the low-lying levels makes the lifetime analysis much more difficult, if not impossible. In practice this becomes a serious limiting factor on the number of lines for which transition probabilities may be found, allowing only those lines having an upper level lying close to the ionization limit to be analyzed, unless the cascading effects may be specifically determined.

A good review of the possibilities for beam-foil spectroscopy is given by Bashkin (1970). For a discussion of the inherent problems, see Oona and Bickel (1970), and Wiese (1970).

THEORY

If two or more quantum states are coupled by an interaction Hamiltonian, H^{int}, there exists a probability that a transition will take place between any two of these states. According to time-dependent perturbation theory, the transition probability per unit time, $w(i \to f)$, is given to first order by:

$$w(i \to f) = \frac{2\pi}{\hbar} \rho \left| \langle f | H^{int} | i \rangle \right|^2 \tag{1}$$

where $|i\rangle$ and $|f\rangle$ are the initial and final quantum states respectively, and ρ is the density of final states.

For radiating systems, the interaction Hamiltonian specifies the interaction of radiation with matter. In the particular case of electric dipole transitions, the spontaneous transition probability can be given in the form:

$$w(i \to f) = \frac{4}{3} \frac{k^3}{\hbar} \left| \langle f | Q_m^1 | i \rangle \right|^2 \tag{2}$$

In this equation, $k = 2\pi/\lambda$, λ is the wavelength of the emitted photon, and Q_m^1 is the electric dipole operator.

To be more specific, let the initial and final states be specified by angular momentum quantum numbers J and M and additional quantum numbers α:

$$|i\rangle \equiv |\alpha' J' M'\rangle$$

$$|\ \rangle \equiv |\alpha J M\rangle$$

In terms of these quantum numbers, the transition probability for spontaneous emission is:

$$w(\alpha'J'M' \rightarrow \alpha JM) = \frac{4}{3}\frac{k^3}{\hbar} \left| \langle JM | Q_m^1 | \alpha'J'M' \rangle \right|^2 \tag{3}$$

By use of the Wigner-Eckart theorem, the above matrix element may be written in terms of a reduced matrix element (the "physical" part) independent of the M-values, and a Clebsch-Gordan coefficient which depends on the M-values (the "geometrical" part).

$$\langle \alpha JM | Q_m^1 | \alpha'J'M' \rangle = \frac{(J'M', 1m | JM)}{\sqrt{2J+1}} \langle \alpha J || Q^1 || \alpha'J' \rangle \tag{4}$$

In the absence of a strong magnetic field, the Zeeman components of a line are not resolved, since the states of different M are degenerate. If the various M states are equally populated, an observed line corresponding to a transition between the two levels J and J' will be composed of all the Zeeman components -- transitions between the sublevels M and M' -- that are allowed by the selection rules. We can then define the Einstein transition probability for the line by the relation:

$$\begin{aligned} A_{if} &= S\, w(\alpha'J'M' \rightarrow \alpha JM) \\ &= \frac{4}{3}\frac{k^3}{\hbar}\frac{1}{(2J'+1)} \left| \langle \alpha J || Q^1 || \alpha'J' \rangle \right|^2 \end{aligned} \tag{5}$$

The symbol S represents an average over the initial sublevels M' and a summation over the final sublevels M. The factor (2J'+1) in the denominator is a result of the summation of the squares of the Clebsch-Gordan coefficients. It is commonly denoted by g and is a statistical weighting factor. For the details of the derivation, see Shore and Menzel (1968).

The square of the reduced matrix element is known as the line strength, $S_d(\alpha'J', \alpha J)$.

$$S_d(\alpha'J',\alpha J) \equiv |\langle \alpha J||Q^1||\alpha'J'\rangle|^2$$

Accordingly,

$$A_{if} = \frac{4}{3}\frac{k^3}{\hbar}\frac{1}{2J'+1} S_d(\alpha'J',\alpha J)$$

$$= \frac{2.026 \times 10^{18}}{\lambda^3(2J'+1)} S_d(\alpha'J',\alpha J) \qquad (6)$$

for λ expressed in Ångstroms ($1\text{Å} = 10^{-10}$).

To calculate the line strengths explicitly, coupling schemes must be introduced. The LS coupling scheme is the prescription for coupling the orbital (ℓ) and spin (s) angular momenta of the individual electrons to form total orbital (L) and total spin (S) angular momenta. Then the L and S are coupled to form the total angular momentum J.

A distinction may be made between those electrons which are in closed ℓ-shells and those electrons which are in incomplete ℓ-shells. A closed ℓ-shell has $2(2\ell+1)$ electrons in it, occupying all the quantum states allowed by the Pauli exclusion principle. Therefore the total L and S are equal to zero.

For the other electrons in incomplete ℓ-shells, there will be a non-zero total L and S. Spectroscopists commonly use LS-genealogy to describe multi-electron atoms. In this prescription, each additional electron couples to a core formed by the other electrons. For a given number of electrons, say eight as in the case of neutral iron, seven of the electrons are coupled to form a total core orbital angular momentum L_c and the eighth electron couples to that core.

$$L_c + \ell = L$$

The outer electron makes transitions from ℓ to ℓ' in accordance with the selection rule that $\Delta\ell = 1$, while the core remains the same.

In the LS coupling scheme, the line strength is given by:

$$S_d = |\langle \alpha SLJ || Q^1 || \alpha' S'L'J' \rangle|^2$$

Following the treatment of Shore and Menzel (1968), this may be expressed in terms of two factors -- R_{mult} and R_{line} -- which give the relative strengths of different multiplets and different lines within a multiplet, respectively.

$$S_d(\alpha SLJ \rightarrow \alpha' S'L'J') = (R_{line})^2 (R_{mult})^2 (\ell_>) [\int P_{n\ell}(r) P_{n'\ell'}(r) dr]^2 \qquad (7)$$

In this equation, $r^{-1}P_{n\ell}(r)$ is the radial part of a one-electron wavefunction and $\ell_>$ is the larger of ℓ and ℓ'. The line and multiplet factors are given explicitly by:

$$R_{line}(SLJ, S'L'J') \equiv \sqrt{(2J+1)(2J'+1)}\, W(SJL'1;1J')$$

$$R_{mult}(L_c L, L_c' L') \equiv \sqrt{(2L+1)(2L'+1)}\, W(L_c L \ell' 1; \ell L') \delta_{cc'}$$

where the W are the Racah coefficients. The selection rules on J and L ($\Delta J = -1,0,+1$ and $\Delta L = -1,0,+1$) follow directly from the properties of these coefficients. For LS coupling, there is a further restriction that $\Delta S = 0$ since the electric dipole operator does not depend on spin.

Finally, the transition probability may be written as:

$$A_{if} = \frac{2.026 \times 10^{18}}{\lambda^3 (2J'+1)} (R_{line})^2 (R_{mult})^2 (\ell_>) [\int P_{n\ell}(r) P_{n'\ell'}(r) dr]^2 \qquad (8)$$

Since the purpose of this experiment is to measure lifetimes of atomic energy levels, it must be shown that a relationship exists between the mean lifetime of the level and the transition probability for a particular transition.

Consider the spontaneous transition of an electron between an initial state i and a lower final state f. The intensity of the resulting spectral line is governed by two factors. The first is the initial population of the state, N_i, which is simply the number of atoms per unit volume in a given quantum state i. The second is the spontaneous transition probability, A_{if}, for the transition between states i and f.

$$I_{if}(t) = A_{if}N_i(t) \tag{9}$$

A quantity often used instead of the transition probability is the oscillator strength, f_{fi}.

$$f_{fi} = \frac{m_e c\lambda^2}{8\pi^2 e^2} \frac{g_i}{g_f} A_{if} = 1.5\ \lambda^2 \frac{g_i}{g_f} A_{if} \tag{10}$$

where g_i and g_f are the statistical weights of the upper and lower levels respectively and λ is given in Ångstroms. This relation is found by comparing the absorption coefficients obtained by a classical and a quantum-mechanical treatment of the absorption of electromagnetic radiation passing through a very rarefied gas. The number of classical oscillators, N_c, that will absorb the same energy as N_i atoms in the state i is given by:

$$N_c = f_{fi}\ N_i$$

In other words, N_c classical oscillators are equivalent to $f_{fi}N_i$ quantum-

mechanical oscillators. The details of the derivation may be found in Foster (1964) or Ziock (1967).

As electrons make spontaneous transitions from an upper level to lower levels, the upper level becomes depleted. The rate of decay of the state i into all lower states f is given by:

$$\frac{dN_i(t)}{dt} = N_i(t) \sum_f A_{if} \tag{11}$$

for the ideal case of absence of absorption, induced emission, collisional effects, and repopulation by cascading from higher levels. Direct integration of Eq. (11) yields:

$$N_i(t) = N_i(0) \exp[-(\sum_f A_{if})t] \tag{12}$$

where $N_i(0)$ is the population of state i at time t = 0. The mean lifetime of the state i is then defined as:

$$\tau \equiv \frac{\int_0^\infty N_i(t)\,t\,dt}{\int_0^\infty N_i(t)\,dt} = \frac{1}{\sum_f A_{if}} \tag{13}$$

which is the time during which the population of state i diminishes to 1/e of its original value. A measurement of the mean lifetime of the state thus gives a direct measurement of the absolute transition probability if there is only one strong transition that contributes significantly to the summation. For more than one strong transition, branching ratios may be used to determine the absolute transition probability.

The ideal case discussed above is not always realizable in a beam-foil experiment. The most serious obstacle is repopulation of the initial state by cascading. This occurs when the upper level lies at a fairly low excitation potential and transitions from higher levels are allowed. In this case, the depletion of the state N_i is less rapid, being governed by the equation:

$$\frac{dN_i(t)}{dt} = \sum_k N_k(t)A_{ki} - N_i(t)\sum_f A_{if} \tag{14}$$

For the simplest case where only one level cascades into the state of interest, the differential equation for the depletion of state N_i is:

$$\frac{dN_i(t)}{dt} = A_{ki}N_k(t) - N_i(t)\sum_f A_{if} \tag{15}$$

Assuming that the kth level decays by Eq. (11), the solution of this equation gives (Wiese 1968):

$$\begin{aligned} N_i(t) = {} & \left[N_i(0) - \frac{A_{ki}N_k(0)}{\sum A_{if} - \sum A_{kl}}\right] \exp\left[-\left(\sum A_{if}\right)t\right] \\ & + \left[\frac{A_{ki}N_k(0)}{\sum A_{if} - \sum A_{kl}}\right] \exp\left[-\left(\sum A_{kl}\right)t\right] \end{aligned} \tag{15}$$

Therefore, the decay rate for the level i would be observed as a sum of two exponential decays. This may be continued for more cascading levels to give sums of more exponentials.

For future reference, a short summary of spectroscopic notation will be useful. The exact specification of the n and ℓ quantum numbers of the electrons is known as the configuration. For example, two electrons in the 1s shell, two in the 2s shell, and three in the 2p shell has the configuration $1s^2 2s^2 2p^3$. The specification of the total S and L of the core is called the parentage, e.g. ^4F. A transition can be fully described by giving the configuration and parentage of the core and the outer coupled electron for both the initial and final states. As an example,

$$3d^7(a^4F)4s - 3d^7(a^4F)4p$$

describes a closed core of seven 3d electrons coupled to form an (a^4F) parent with the outer electron making a transition from a 4s to a 4p state. The a in (a^4F) denotes the exact way in which the seven electrons are coupled to form the ^4F core.

The designation is the result of the coupling of the outer electron to the core. One possibility for the above transition would be:

$$a^3F_4 - z^3G^\circ_5$$

The superscript $^\circ$ indicates odd parity.

EXPERIMENTAL PROCEDURE

A beam of Fe^+ ions were accelerated into a thin carbon foil to produce a glowing beam of primarily neutral iron in various levels of excitation. A wavelength scan was taken to identify the lines present. Decay curves were then taken of the strongest lines by moving the foil holder upstream while keeping the monochromator fixed in position. The decay curves were multi-scaled into a multi-channel analyzer for subsequent print-out and analysis. A diagram of the apparatus is shown in Plate I.

The iron beam was produced in a Physicon Model 910 universal ion source by passing hot CCl_4 gas over an iron wire and extracting the iron ions, along with others produced, from the plasma. They were then accelerated electrostatically to an energy ranging from 70 to 100 keV. Since several different components of the beam existed, in particular several isotopes of chlorine, the beam was mass-analyzed by passing through an analyzing magnet. To calibrate the magnet, an argon beam was first produced by introducing argon gas into the source. A Hall probe was used to find the relative strength of the magnetic field. Since the ratio of the magnetic fields needed to bend two different beams of the same energy along the same radial path is inversely proportional to the ratio of the square root of the masses, the magnetic field needed to pass a beam of mass 56 down the beam line could be calculated.

After being mass and energy analyzed, the Fe^+ beam passed through a 5 mm circular collimator and then into the target chamber where it passed through the carbon foil. The foils were very thin, ranging from approximately 1 to 4 $\mu g/cm^2$. For the majority of the lifetime data, the foils used were prepared at the University of Arizona and were of nominal thickness 2.5 $\mu g/cm^2$. These foils are very delicate and must be supported in some manner. To pro-

vide support, they were mounted on an electroplated nickel mesh with a .25 mm grid spacing, which transmitted approximately 80% of the beam. For wavelength scans, 4 $\mu g/cm^2$ foils were used, as they were capable of withstanding the 0.5 to 1 μA beam currents for an hour or longer without appreciable deterioration. Thinner 2.5 $\mu g/cm^2$ foils were used for lifetime data and they typically deteriorated badly within half an hour or less.

The foils were attached to a circular disc which could be rotated to change foils during a run as they deteriorated. Wavelength scans were accomplished by focusing the slits of the monochromator immediately downstream of the foil where the beam was most intense. The monochromator scanned the wavelength region at a constant rate, typically 50 Å/min.

For recording decay curves, the foil holder was scanned upstream and back downstream in a continuous 30-second cycle with the monochromator fixed in position. The distance scanned in one direction was typically 6.55 cm. Fluctuations in the beam current will adversely affect lifetime data unless they are specifically taken into account. This was accomplished by scanning the foil continuously for 10 to 15 cycles to average out fluctuations in the beam current. At the same time, the beam current was collected in a Faraday cup located at the end of the chamber and monitored on a Keithley picoammeter to be sure that the beam current did not fluctuate by a large amount.

The monochromator used was a McPherson Model 218 with a 0.3 m focal length and a speed of f/5.3. The entrance slits were focused perpendicular to the beam by a LiF lens with a focal length of 4.5 in. at 3000 Å and 4.68 in. at 5000 Å. The grating had 2400 lines/mm with a dispersion of 13.3 Å per mm.

Photons of the proper wavelength to pass through the exit slits of the

monochromator were detected by an EMI-6256S photomultiplier tube operated in the pulse-counting mode. To reduce the dark count of the tube, it was encased in a copper sleeve with a cold finger extension which was cooled in a dry-ice slurry. Later the cooling arrangement was modified by using a thermo-electric cooling module attached to the cold finger, which greatly simplified the cooling process. After being cooled, the tube had a dark count of 1 to 2 counts per second.

The negative pulses from the anode of the PMT ranged from 0.5 to 2 mV with a 20-μsec decay constant. The pulses were clipped at 2 μsec and then amplified by a Nuclear Data duel amplifier Model ND 500. A lower level discriminator was set to eliminate very low-voltage noise pulses that were not related to photons incident on the photocathode. Standard 5-volt, 2-μsec pulses were generated by the amplifier-discriminator and multi-scaled into a Technical Measurement Corporation 400 channel multi-channel analyzer, Model 404-6.

In taking lifetime data, the TMC was synchronized with the foil scanner in such a way that at the end of each scanning cycle, the multi-channel analyzer reset to the first channel to continue collecting counts. In this way the foil could be scanned until at least 1000 counts were accumulated at the peak of the decay curve. The wavelength scans were taken by scanning the monochromator at a constant rate while stepping the analyzer at 1 channel/sec. The plotted data then showed a linear relationship between channel number and wavelength. By starting the monochromator scan and the analyzer simultaneously, the output could then be calibrated. The stored data was then typed out to be analyzed and plotted.

LINE IDENTIFICATION

The spectrum of FeI for the wavelength region from 3700Å to 4450 Å is shown in Plate II. Because of the low intensity of the glowing beam, the monochromator slits were set for 0.2 mm, introducing a line width of 2.7 Å from the dispersion of the grating. The observed line width (FWHM) was 3.2 Å. Due to the complexity of the neutral iron spectrum, there may be more than one line present in a width of this size. (Corliss and Tech 1968, hereafter referred to as CT, list an average of more than one line per Å in this region of the spectrum.) This may make line identification difficult.

To make the identifications, the strongest lines were first assigned a wavelength within approximately 1 Å by the direct correlation between channel number and wavelength. These wavelengths were then located in the tables of CT. A strong correlation was found to exist between those lines listed in CT with large gA values and the strong lines in the spectrum. This allowed a final identification of the lines as those with the proper wavelength having a larga gA value. A further criterion for identification was to find several members of a multiplet in approximately the expected intensity ratios. After several definite identifications were made, the rest of the lines could be identified to within approximately 0.1 Å by calibrating the spectrum to the strong lines.

In case a strong spectral line might include two or more lines listed in CT with large gA values, a search was conducted for other members of the multiplets. If one multiplet series was strong and the others either not present or very weak, then the strong line could confidently be identified as a member of the strong multiplet, with the others contributing negligibly.

It was not always possible to rule out the presence of more than one line.

The spectrum shown in Plate II gives the multiplet identifications corresponding to the classification of Moore (1959). All the identified members of a given multiplet are enclosed in brackets. The vertical lines on the abscissa indicate the approximate magnitudes of the gA values of CT. The numbers above the lines are for identification purposes relative to Table I. The group of lines just below 3760 Å could not be identified unambiguously due to the large number of possible lines with large gA values. Many weak lines throughout the spectrum also could not be definitely identified.

Table I gives the identifications that have been made corresponding to the numbers on the spectrum, with the respective gA values of CT and the multiplet designation of Moore. A good example of the identification procedure is the line at 3806 Å. According to Table I, there are two lines of different multiplets that both have a large gA. By referring to other members of multiplets 607 and 608 seen in the spectrum and comparing relative intensities with gA values, one would expect that the 3806 Å line is largely from multiplet 608, with the 607 component being relatively small. The line at 4143 Å is also difficult to interpret at first glance since there are no other members of the 523 multiplet for comparison. Comparing other lines of multiplet 43, however, it is seen that the intensity of line 16 is approximately three times greater than would be expected from that component of multiplet 43. It is expected, therefore, that the major contribution must come from multiplet 523, but that multiplet 43 also contributes a significant part of the intensity.

The electronic configurations and the term designations for the identified lines are given in Table II. All of the transitions observed are of

the form $3d^7 4p \rightarrow 3d^7 4s$, with the parent ion configuration unchanged.

A Grotrian diagram of FeI is shown in Plate III. The levels are identified by multiplicity and by total orbital angular momentum L. The various J-values are not distinguished. The levels are plotted as a function of wavenumber in kK (1 kK = 10^3 cm^{-1}). FeI has 18 electrons in closed ℓ-shells with 8 electrons in incomplete shells. These 8 electrons couple in many complex ways to form the complicated energy level diagram of Plate III. The configuration of the closed core is $1s^2 2s^2 3p^6 3s^2 3p^6$ and the ground state is $3d^6 4s^2\ {}^5D_4$. The ionization potential is 63.7 kK or 7.90 ± 0.01 eV. The information for producing this Grotrian diagram was taken from Atomic Energy Levels by Moore (1952).

The transitions identified in the spectrum are indicated by multiplet number in the energy level diagram. It is interesting to note that two strong intersystem transitions have been seen. This indicates that LS coupling is not entirely applicable in the case of neutral iron. It is apparent that cascading will be a major problem for lines in multiplets 41, 42, 43, and 45. The possible cascading lines into multiplet 43 have been indicated on the diagram. This will be discussed more extensively in the section on cascading.

LIFETIME ANALYSIS

The measurement of the mean lifetime of an excited state by the beam-foil method is reduced to observing the decay in intensity of a spectral line as a function of distance from the foil. The distance can be directly translated into the time after the excitation process occurred since the velocity of the beam is determined from the post-foil velocity.

$$t = \frac{x}{v} = \frac{x}{\sqrt{2E/m}} \tag{16}$$

for the non-relativistic velocities of this experiment. From equations (11) and (13),

$$\frac{dN_i(t)}{dt} = -\frac{1}{\tau}\,dt \tag{17}$$

which may be directly integrated to give:

$$\ln N_i(t) = -\frac{1}{\tau}\,t + \ln N_i(0) \tag{18}$$

The lifetime τ is the slope of the line of a logarithmic plot of the number of counts as a function of distance (time).

In order to determine the lifetime, the post-foil velocity of the beam must be determined. In passing through the foil, the beam particles lose energy by charge exchange and elastic nuclear collisions, and this must be accounted for in finding the beam velocity. Bohr (1913) first suggested that the energy loss of an ion could be attributed to two effects: nuclear stopping and electronic stopping, the total stopping power being the sum of

these two factors. Electronic energy loss is attributable to the exchange and capture of electrons by the two atoms and is the dominant effect at high energies. The nuclear stopping is caused by elastic collisions between the screened nuclei of the target and incident atoms and is dominant at the low energies of this experiment.

The various theoretical approaches used to calculate the energy loss are summarized in the review article by Northcliffe (1963). Lindhard, Scharff, and Schiott (1963) have derived a universal curve for nuclear stopping power and give an equation for calculating electronic stopping power at low energies ($\beta < Z_1^{2/3}/137$ where Z_1 is the incident ion atomic number).

$$S_e = \xi_e \, 8\pi e^2 N a_0 \frac{Z_1 Z_2}{(Z_1^{2/3} + Z_2^{2/3})^{3/2}} 137\beta \qquad (19)$$

in which a_0 is the Bohr radius, ξ_e is a constant of the order of $Z_1^{1/6}$, and N is the number of atoms per unit volume.

Using the results of Lindhard, et.al., the calculated energy loss for a 70 keV beam of neutral iron incident on a 2.5 $\mu g/cm^2$ carbon foil was 18.2 keV, of which 11.8 keV was due to nuclear energy loss. For a 100 keV beam, the loss was 17.2 keV, nuclear effects contributing 10.5 keV. The largest uncertainty in this calculation is the actual thickness of the foil. The foils were obtained from the University of Arizona and Stoner (1969), from the University of Arizona, has determined that there is a large non-carbon component to the foils. Work currently being done at Kansas State University by J. Brand to determine the beam velocity by Doppler shift and electrostatic deflection methods indicates that the velocity determination based on the energy loss in the foil may be in error by as much as 10%.

The total length of the scan for taking lifetime data was 6.55 cm. One

must be careful that part of the beam does not scatter out of the acceptance field of the monochromator in this distance, or the observed decay curve would decrease too rapidly, yielding a lifetime shorter than the actual value. Högberg, Nordén, and Berry (1970) have studied the problem of angular distributions of ions scattered in thin carbon foils and concluded that for energies between 10 and 100 keV and for carbon foils thinner than $2\sqrt{Z_{ion}}$ $\mu g/cm^2$, the angular distribution is a Gaussian with a halfwidth $\Psi_{1/2}$ given by:

$$\Psi_{1/2} = 12.0\ (Z_{ion}^{3/4}\ t/\bar{E}) \tag{20}$$

where t is the thickness of the foil in $\mu g/cm^2$, $\bar{E}$ is the mean energy in keV, and $\Psi_{1/2}$ is given in degrees. Calculations using this equation show that for lifetimes on the order of 10 nsec, the scattering should be a contribution of less than 1%, though for very long lifetimes, it could become significant. Since the diameter of the photocathode is only 10 mm, the focusing lens was set to magnify the image of the photocathode on the beam by a factor of 1.7, which greatly reduces the possibility of scattering out of the acceptance field.

The decay curve for each line was analyzed by a least squares fit to a two-exponential function plus a dark count (DK).

$$I(t) = A \exp(-t/\tau_1) + B \exp(-t/\tau_2) + DK \tag{21}$$

The dark count was recorded when taking the data, so it was known and was therefore not entered as a variable. The fitting program[1] calculated the

---

[1]The assistance of Ron Keller in helping write the least-squares fitting program is gratefully acknowledged.

values of A, B, τ_1, and τ_2 for the fit that minimized chi-square.

It has been noted (Oona and Bickel 1970; Carré et.al. 1970) that the results of a curve-fitting procedure are subject to large error if, for example, a two-exponential function is fitted to a curve that in fact contains three exponentials. A good fit can be obtained but the result will be too high for the shortest lifetime and too low for the longest lifetime. It is therefore imperative to understand the level structure and the cascading lines that are present.

There are two limiting cases where the cascading problem may be minimized. Cascades become negligible if their lifetimes are either extremely long or extremely short compared to the transition of interest and may be neglected. If the cascades have lifetimes reasonably different from that of the transition being analyzed. they may frequently be included in a single effective exponential and a two-exponential fit can then be made. To be able to analyze lines with cascading components, then, one must analyze the situation very carefully.

CASCADING

Referring to the Grotrian diagram of Plate III showing the multiplet transitions seen, it is apparent that cascading from upper levels may be a serious problem for lines in multiplets 41, 42, 43, and 45, all of which have their upper level lying at a low excitation potential.

In all of the transitions identified, the parent ion configuration is unchanged while the outer electron jumps from a 4p to a 4s state. Therefore one may expect that fairly strong cascading transitions would be those having the same core but with the outer electron jumping from a 4d to a 4p state.

With this assumption, relative transition probabilities were calculated using Eq. (8) for all lines listed in Atomic Energy Levels (1952) satisfying the selection rules for transitions into the upper levels of multiplets 41, 42, 43, and 45 where the electron making the transition was a 4d electron. In this case the radial factor in Eq. (8) cancels out in the ratio of two transition probabilities since it is the same for all 4d - 4p transitions, and relative transition probabilities can be determined, normalized to unity for the strongest transition calculated. There are several 5s - 4p transitions, but the radial factors will not cancel then, so relative transition probabilities could not be calculated for these transitions. By knowing the relative gA values, one could then look for the strongest cascading lines and find their intensities relative to the intensities of the line under consideration. In this way it would be possible to consider the cascading lines in finding the lifetime of the state being analyzed.

These calculations were done under the assumption that intersystem transitions would not be an important consideration. However, the fact that two

strong multiplets are seen that violate this selection rule leads one to believe that it would also be violated for the cascading lines. A complete search was made in the tables of CT for all lines listed with their final level being the same as the upper level for the lines seen in multiplets 41, 42, 43, and 45. The results of this analysis for the six lines in these multiplets for which lifetime data is taken, are presented in Table III. It is immediately apparent that many intersystem transitions exist and further that many have large gA values. This makes the cascading analysis very difficult.

Whether or not the cascading is an important contribution depends critically on the population of the 4d and 5s states, by Eq. (9). Previous beam-foil work done in this laboratory by Brand, Cocke, and Curnutte have given some indication that 4d levels may not be heavily populated in the collisional excitation process in Cr. This may be checked in the case of Fe by directly measuring the intensities of some of the strong lines. It is also possible that the various levels cascading into the level of interest could be included in a single effective exponential, thus being amenable to analysis.

The actual measurement of the intensities of the strongest cascading lines has not yet been done, as they lie in a higher wavelength region from that of this experiment and the present detection system is not efficient in that region. It is hoped that this analysis can be done in the near future with the use of a more efficient grating.

RESULTS AND CONCLUSIONS

The decay curves and the least-squares fits calculated by the computer program for the lines amenable to analysis are shown in Plates IV - XIV. All of the curves were fit to two exponentials plus a dark count and the lifetimes of both decay curves are shown on the graphs. The constant dark count was not included in the graph, though it was 3 to 4 counts per channel for most of the curves. All the lines analyzed had a strong short-lived component plus a weak component with a lifetime of two to four times longer. The lines in multiplets 522, 523, 608, 800, and 801 all have their upper levels lying close to the ionization limit, making it very improbable that cascading is an important consideration. Indeed, Corliss and Tech list no lines that make transitions into these levels. Therefore, the weak long-lived component is probably the result of a low-level underlying background of other lines with an effective long lifetime.

The lines in multiplets 42 and 43 are not so easily analyzed because of the cascading problem previously discussed. The 4045.8 Å line has a very weak cascading component with a very long lifetime. It appears that the many possible cascading components listed in Table III do not have a large effect on the main decay curve. The lines at 4063.6 Å and 4071.7 Å have a stronger cascading component with a shorter effective lifetime. All of the lines with cascading components could be fit very well with a two-exponential decay scheme. However, as was mentioned previously, a three-exponential decay analysis might also be able to fit the data equally well. For this reason, the lifetimes for these lines were assigned an accuracy of 30%, pending further analysis that might shed some more light on the cascading problem.

The lifetimes that were obtained are given in Table IV. The probable errors were assigned from an estimated uncertainty of 10% in the beam velocity for all the lines and an additional 20% uncertainty for the lines with a high probability of significant cascading. The lifetimes are compared with the results of various other experiments. Of particular interest is the very good agreement with the lifetimes obtained by Whaling et.al. using the beam-foil technique but with energies ranging from 200 to 1500 keV and with 10 $\mu g/cm^2$ foils. The comparisons with CT and CB are of interest because of the widespread use of these tables by astrophysicists. The CT and CB lifetimes were obtained by taking the reciprocal of the sum of transition probabilities from the upper level to all lower levels according to Eq. (13). The ratio of the lifetimes measured in this experiment to the CT and CB lifetimes varies from 2.3 to 10, a rather significant variation. It is particularly interesting to note that the variation of the CT lifetimes appears to depend on the upper excitation level, being larger for levels near the ionization potential. This is consistent with the results of several other recent experiments, as was mentioned in the Introduction.

To allow a direct comparison of the results of the various experiments, the difference in the log of the gf-values for a given experiment and those of CT was determined. These differences are tabulated in Table IV, where Δlog gf is defined as $\log gf_{CT} - \log gf_{other}$. They are also plotted as a function of upper level excitation in Plate XV. All of the experiments compared indicate an increasing difference in gf-values with respect to CT for higher energy levels. This indicates that there may be an error in the CT gf-values which has a systematic dependence on the excitation energy of the upper level.

To draw firm conclusions about any systematic trends of the variation

of gf-values or lifetimes with respect to excitation level depends on the availability of much more experimental data covering a larger region of excitations. There is a definite need for more experiments to be done in this area to pin down the lifetimes and transition probabilities more exactly. In particular, the cascading problem needs to be studied in great detail to allow a more accurate determination of the lifetimes of many more levels. Further work needs to be done on the problem of energy loss in the foil to determine the post-foil beam velocity more accurately or the problem could be avoided altogether by finding other methods to determine the velocity.

BIBLIOGRAPHY

Bashkin, S., Nucl. Instr. & Meth. 90, 3 (1970)

Bashkin, S., L. Heroux, and J. Shaw, Phys. Letters 13, 229 (1964)

Bashkin, S., P.R. Malmberg, A.B. Meinel, and S.G. Tilford, Phys. Letters 10, 63 (1964)

Bashkin, S. and A.B. Meinel, Ap. J. 139, 413 (1964)

Bohr, N., Phil. Mag. 25, 10 (1913)

Bohr, N., Mat. Fys. Medd. Dan. Vid. Selsk. 18 (1948)

Clayton, D.D. Principles of Stellar Evolution and Nucleosynthesis. (McGraw-Hill, N.Y.) 1968

Corliss, C.H. and W.R. Bozman, N.B.S. Monograph, No. 53 (1962)

Corliss, C.H. and B. Warner, Ap. J. Suppl. 8, 395 (1964)

Corliss, C.H. and J.L. Tech, N.B.S. Monograph, No. 108 (1967)

Foster, E.W., Reports on Progress in Physics 27, 469 (1964)

Garz, T. and M. Kock, Astron. Astrophys. 2, 274 (1969)

Grasdalen, G.L., M. Huber, and W.H. Parkinson, Ap. J. 156,1153 (1969)

Högberg, G., H. Nordén, and H.G. Berry, Nucl. Instr. & Meth. 90, 283 (1970)

Huber, M.C.E. and W.H. Parkinson, Harvard College Obs. SR-34 (1971)

Huber, M.C.E. and F.L. Tobey, Ap. J. 152, 609 (1968)

Lindhard, J., M. Scharff, and H.E. Schiott, Mat. Fys. Medd. Dan. Vid. Selsk. 33, No. 14 (1963)

Moore, C.E., Atomic Energy Levels (1952)

Moore, C.E., PB 151 395 (U.S. Dept. of Commerce, Washington, D.C.) 1959

Motz, L. Astrophysics and Stellar Structure. (Ginn and Company, Waltham, Mass.) 1970

Müller, E.A. "Abundance Determination in Stellar Spectra" ed. H. Hubenet (London & N.Y., Academic Press) 1966, p. 171

Northcliffe, L., Ann. Rev. Nucl. Sci. 13, 67 (1963)

Oona, H. and W.S. Bickel, Nucl. Instr. & Meth. 90, 223 (1970)

BIBLIOGRAPHY

(Cont'd)

Shore, B.W. and D.H. Menzel. Principles of Atomic Spectra. (John Wiley & Sons, Inc., New York), 1968

Stoner, J.O. and L.J. Radziemski, Nucl. Instr. & Meth. 90, 275 (1970)

Watson, W.D., Ap. J. (Letters) 158, L189 (1969)

Whaling, W., R.B. King, and M. Martinez-Garcia, Ap. J. 158, 389 (1969)

Whaling, W., M. Martinez-Garcia, D.L. Mickey, and G.M. Lawrence, Nucl. Instr. & Meth. 90, 363 (1970)

Wiese, W.L. Methods of Experimental Physics, Vol. 7, Part A. (Academic Press, London) 1968, p. 117

Wiese, W.L., Nucl. Instr. & Meth. 90, 25 (1970)

Wolnik, S.J., R.O. Berthel, and G.W. Wares, Ap. J. 162, 1037 (1970)

Ziock, K. Methods of Experimental Physics, Vol. 4, Part B (Academic Press, London), 1967

Bridges, J.M. and W.L. Wiese, Ap. J. 161, L71 (1970)

THIS BOOK CONTAINS NUMEROUS PAGES THAT WERE BOUND WITHOUT PAGE NUMBERS.

THIS IS AS RECEIVED FROM CUSTOMER.

EXPLANATION OF PLATE I

Experimental Arrangement for Beam-Foil Experiment

THIS BOOK CONTAINS NUMEROUS PAGES WITH DIAGRAMS THAT ARE CROOKED COMPARED TO THE REST OF THE INFORMATION ON THE PAGE.

THIS IS AS RECEIVED FROM CUSTOMER.

EXPERIMENTAL ARRANGEMENT

PLATE I

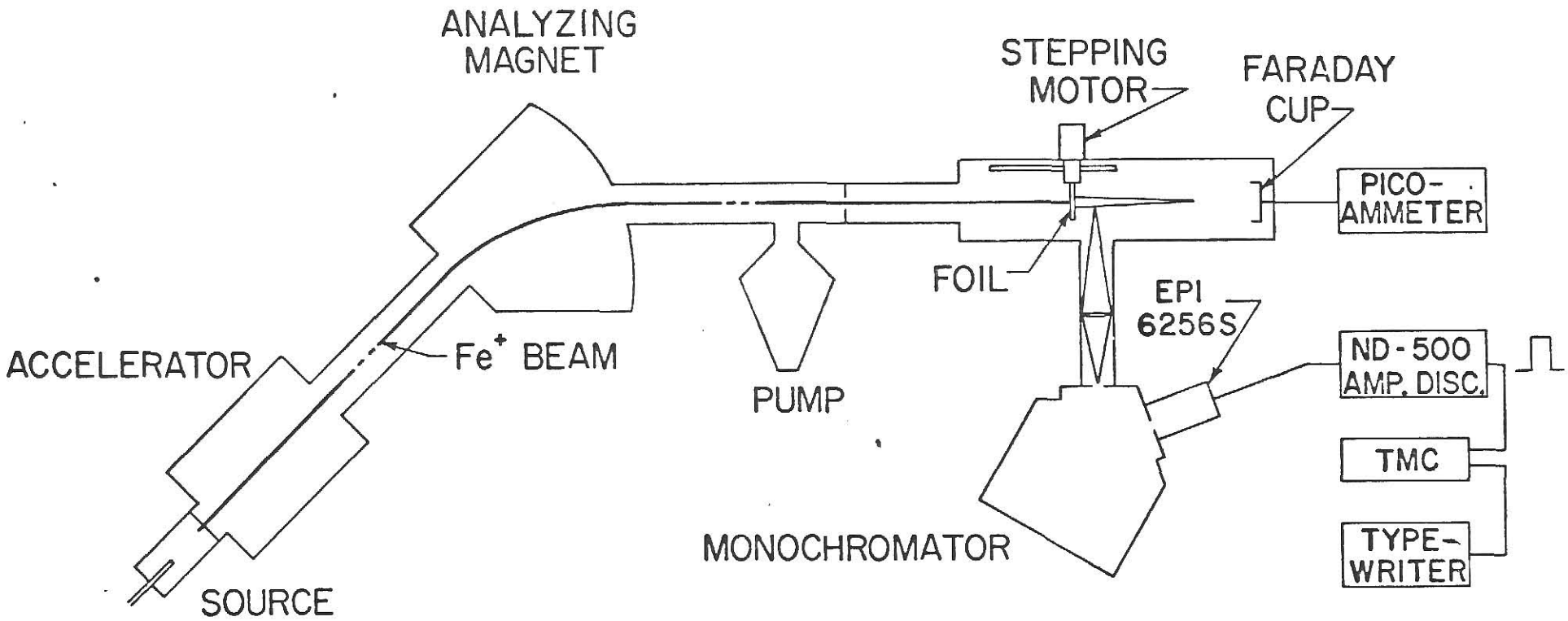

EXPLANATION OF PLATE II

Beam-Foil Spectrum from 70 keV FeI. The bracketed lines are the multiplet identifications of Moore (1959). The vertical lines on the abscissa indicate the approximate gA values of CT. The lines are identified in Table I according to the sequential numbers above the lines.

PLATE II

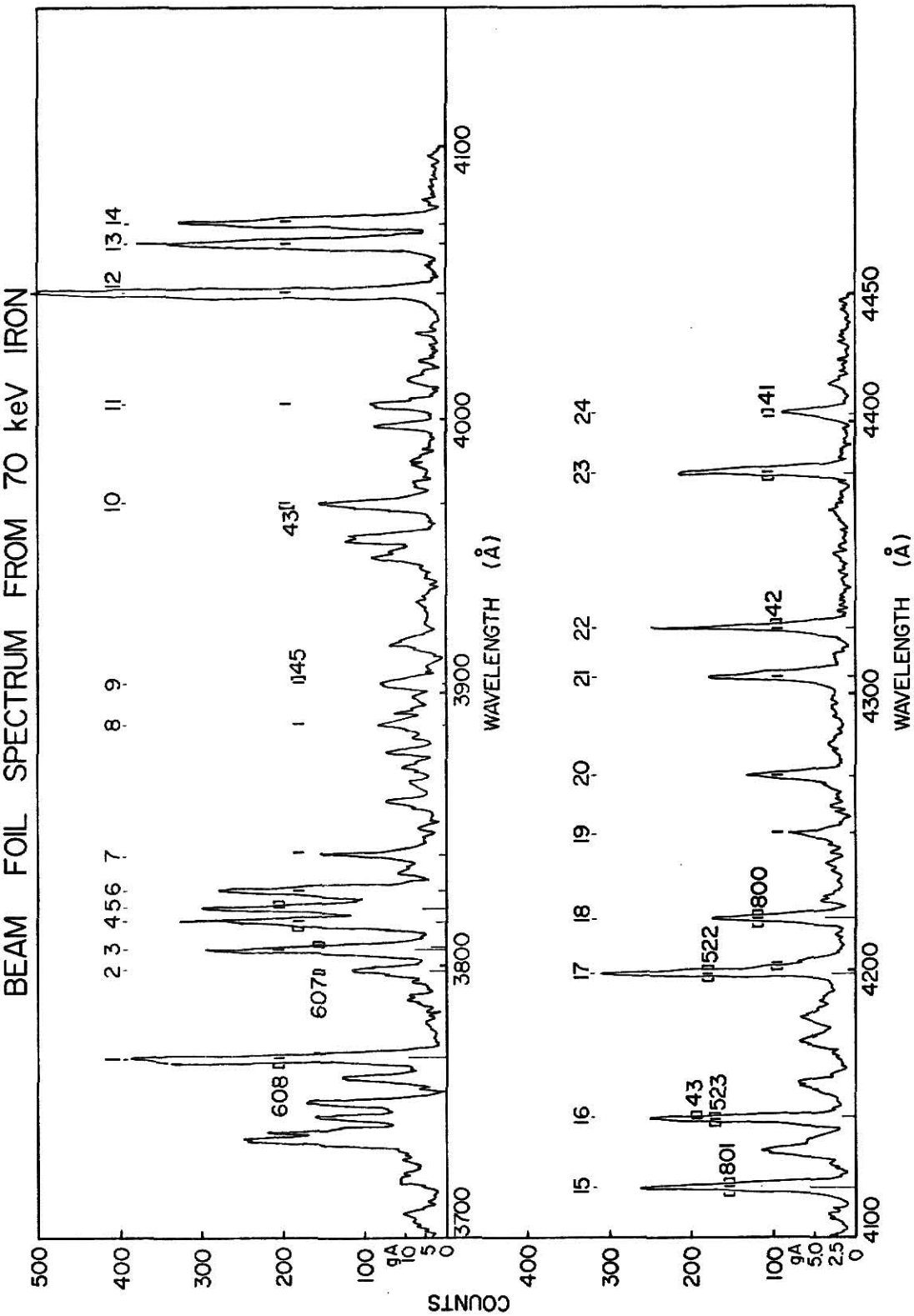
BEAM FOIL SPECTRUM FROM 70 keV IRON
COUNTS
WAVELENGTH (Å)
WAVELENGTH (Å)
608
607
431
145
522
800
801
43
523
42
141

EXPLANATION OF PLATE III

Grotrian Diagram of FeI. The transitions identified are indicated by the heavy lines and are classified according to the multiplet number assignment of Moore (1959). The light lines feeding into the upper level of multiplet 43 are the possible cascades into this level. Note the many intersystem transitions.

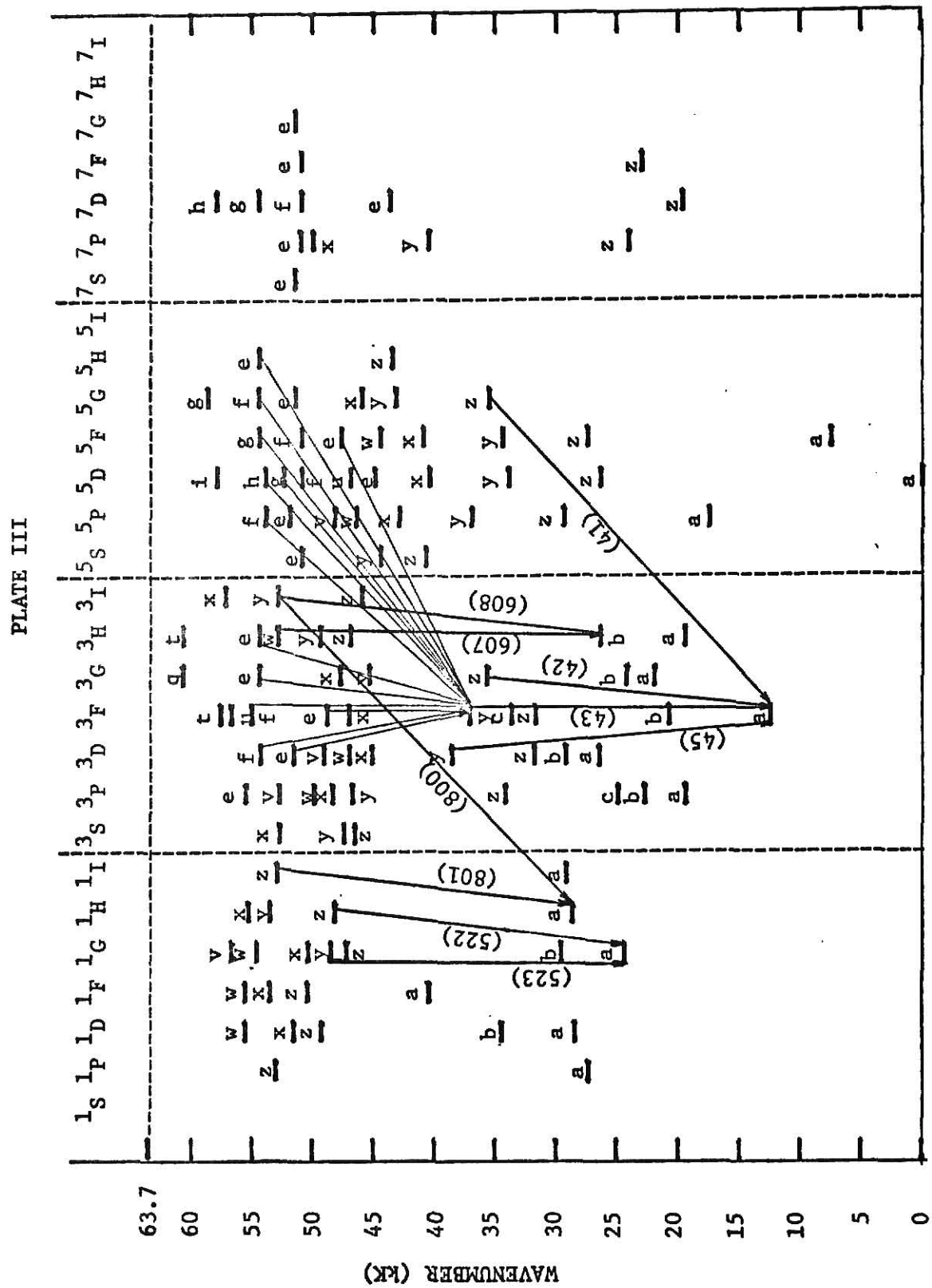
PLATE III
WAVENUMBER (kK)
63.7
60
55
50
45
40
35
30
25
20
15
10
5
0
(801)
(522)
(523)
(800)
(608)
(607)
(42)
(43)
(45)
(41)

EXPLANATION OF TABLE I

Identification of lines in the spectrum. The line number correlates the table to the lines in the spectrum of Plate I. The multiplet number is taken from Moore (1959). The gA values of Corliss and Tech (1967) and Corliss and Bozman (1962) are given.

TABLE I

Line Number	Wavelength (Å)	Multiplet Number[1]	gA X10^9 sec^{-1} CT[2]	gA X10^9 sec^{-1} CB[3]
1	3765.541	608	9.62	5.0
2	3797.517	607	4.18	2.1
3	3805.345	608	7.41	4.5
	3806.699	607	3.48	2.1
4	3815.843	45	1.82	1.6
5	3821.181	608	5.64	2.5
6	3827.826	45	1.62	1.5
7	3841.050	45	1.33	1.0
8	3888.516	45	0.47	0.4
9	3902.948	45	0.45	0.6
10	3969.260	43	0.40	0.4
11	4005.244	43	0.34	0.4
12	4045.815	43	1.86	2.2
13	4063.596	43	1.11	1.0
14	4071.740	43	1.06	0.9
15	4118.548	801	5.68	3.3
16	4143.417	523	1.72	1.6
	4143.870	43	0.30	0.3
17	4199.100	522	2.59	2.5

TABLE I
(Cont'd)

Line Number	Wavelength (Å)	Multiplet Number[1]	gA X10^9 sec^{-1} CT[2]	gA X10^9 sec^{-1} CB[3]
18	4219.360	800	3.85	2.7
19	4250.790	42	0.19	0.2
20	4271.760	42	0.58	0.5
21	4307.900	42	0.75	0.6
22	4325.760	42	0.82	0.6
23	4383.550	41	1.12	0.8
24	4404.750	41	0.61	0.4

[1]Moore (1959)
[2]Corliss and Tech (1967)
[3]Corliss and Bozman (1962)

EXPLANATION OF TABLE II

Electronic configurations and designations for the identified lines. These are taken from Atomic Energy Levels (Moore 1952).

TABLE II

Multiplet[1]	Configurations[2]	Designations[3]	Wavelength
41	$3d^7(a^4F)4s - 3d^7(a^4F)4p$	$a^3F_4 - z^5G^\circ_5$	4383.6
		3 - 4	4404.8
42	$3d^7(a^4F)4s - 3d^7(a^4F)4p$	$a^3F_4 - z^3G^\circ_5$	4271.8
		3 - 4	4307.9
		2 - 3	4325.8
		3 - 3	4250.8
43	$3d^7(a^4F)4s - 3d^7(a^4F)4p$	$a^3F_4 - y^3F^\circ_4$	4045.8
		3 - 3	4063.6
		2 - 2	4071.7
		4 - 3	3969.3
		3 - 2	4005.2
		3 - 4	4143.9
45	$3d^7(a^4F)4s - 3d^7(a^4F)4p$	$a^3F_4 - y^3D^\circ_3$	3815.8
		3 - 2	3827.8
		2 - 1	3841.0
		3 - 3	3902.9
522	$3d^7(a^2G)4s - 3d^7(a^2G)4p$	$a^1G_4 - z^1H^\circ_5$	4199.1
523	$3d^7(a^2G)4s - 3d^7(a^2G)4p$	$a^1G_4 - y^1G^\circ_4$	4143.4

TABLE II
(Cont'd)

Multiplet[1]	Configurations[2]	Designations[2]	Wavelength
607	$3d^7(a^2H)4s - 3d^7(a^2H)4p$	$b^3H_6 - w^3H^\circ_6$	3797.5
		5 - 5	3806.7
608	$3d^7(a^2H)4s - 3d^7(a^2H)4p$	$b^3H_6 - y^3I^\circ_7$	3765.5
		5 - 5	3765.7
		5 - 6	3821.2
		4 - 5	3805.3
800	$3d^7(a^2H)4s - 3d^7(a^2H)4p$	$a^1H_5 - y^3I^\circ_6$	4219.4
801	$3d^7(a^2H)4s - 3d^7(a^2H)4p$	$a^1H_5 - z^1I^\circ_6$	4118.5

[1]Moore (1959)
[2]Moore (1952)

EXPLANATION OF TABLE III

Cascading lines. All the lines given in Corliss and Tech (1967) that make transitions into the upper levels of multiplets 42 and 43 are given in this table. The lines in the first column are those for which decay curves have been analyzed. The designations are from Atomic Energy Levels (Moore 1952). The gA values are given in Corliss and Tech (1967).

TABLE III

Wavelength (Mult.)	Upper Level	Cascade Level	Cascade Wavelength	Mult.	gA X10^9 sec^{-1} CT
4271.8	$z^3G^\circ_5$	f^5G_6	5619.60	1161	0.032
(42)		g^5F_5	5653.89	1143	0.041
		e^5F_5	8598.79	1153	0.014
		4	8331.94	1153	0.110
		e^5H_5	5405.36	1159	0.148
		h^5D_4	5624.06	1160	0.075
		e^3G_5	5445.04	1163	0.483
		4	5349.74	1163	0.037
		e^3H_6	5415.20	1165	1.668
		e^3F_4	7945.88	1154	0.220
4307.9	$z^3G^\circ_4$	f^5G_5	5708.11	1161	0.054
(42)		4	5553.59	1161	0.056
		e^5F_3	8339.43	1153	0.054
		e^3G_5	5562.71	1163	0.088
		4	5463.28	1163	0.420
		e^3H_4	5321.11	1165	0.082
		f^3F_4	5285.13	1166	0.050
		3	5164.56	1166	0.158
		e^3F_4	8198.95	1154	0.050
		3	7832.22	1154	0.204
4045.8	y^3F_4	f^5G_5	6024.07	1178	0.441
(43)		4	5852.19	1178	0.064
		g^5F_4	5983.70	1175	0.125
		g^5D_3	6627.56	1174	0.012
		h^5D_4	5929.70	1176	0.061
		e^5F_4	9350.46	1171	0.035

TABLE III
(Cont'd)

Wavelength (Mult.)	Upper Level	Cascade Level	Cascade Wavelength	Mult.	gA X10^{9} sec^{-1} CT
4045.8 (43)	$y^3F^\circ_4$	e^3G_5	5862.36	1180	0.269
		4	5752.04	1180	0.126
		e^3H_5	5686.53	1182	0.254
		4	5594.67	1182	0.110
		f^3F_4	5554.90	1183	0.227
		e^3F_4	8866.96	1172	0.186
		3	8439.60	1172	0.040
		f^3D_3	5859.61	1181	0.184
		e^3D_3	6843.67	1173	0.059
4063.6 (43)	$y^3F^\circ_3$	f^5G_4	6020.17	1178	0.245
		e^5H_4	5855.13	1179	0.060
		g^5F_3	5997.80	1175	0.051
		e^5F_3	9437.91	1171	0.012
		g^5D_2	6715.41	1174	0.011
		f^5P_2	6093.66	1177	0.027
		e^3G_4	5914.10	1180	0.243
		3	5806.73	1180	0.120
		e^3H_4	5747.96	1182	0.066
		f^3F_4	5705.99	1183	0.290
		3	5565.71	1183	0.327
		e^3F_4	8866.96	1172	0.186
		3	8793.38	1172	0.120
		f^3D_2	5914.10	1181	0.270
		e^3D_2	6858.16	1173	0.052

TABLE III
(Cont'd)

Wavelength (Mult.)	Upper Level	Cascade Level	Cascade Wavelength	Mult.	gA X10^9 sec^{-1} CT
4071.7	$y^3F^\circ_2$	f^5G_3	6007.96	1178	0.110
		g^5D_1	6804.02	1174	0.016
		h^5D_2	6079.02	1176	0.048
		e^3G_3	5930.17	1180	0.399
		f^3F_3	5679.02	1183	0.217
		2	5598.30	1183	0.322
		e^3F_3	9079.60	1172	0.046
		2	8764.00	1172	0.133
		f^3D_1	5905.67	1181	0.115
		e^3D_1	6885.77	1173	0.028

EXPLANATION OF PLATE IV

Decay curve for the line at 3765.5 Å. τ_1 is the lifetime in nsec of the upper level of the line. τ_2 is a long-lived component attributed to unresolved low-intensity lines. The constant dark count was not included in any of these decay curves, although it was included in the computed least-squares fit. It was typically 3 to 4 counts per channel.

PLATE IV

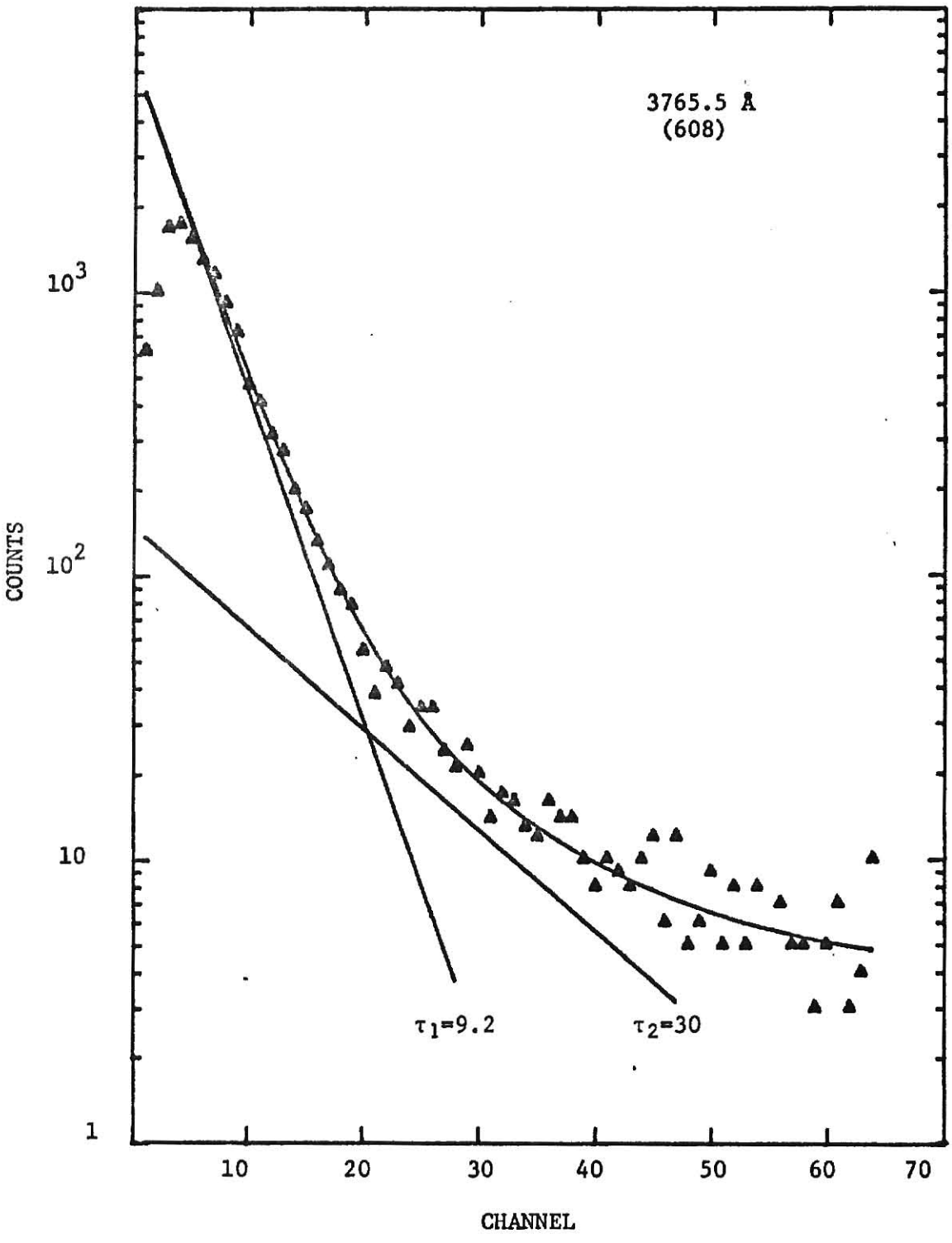
3765.5 Å
(608)
10^3
10^2
10
1
COUNTS
τ_1=9.2
τ_2=30
10
20
30
40
50
60
70
CHANNEL

EXPLANATION OF PLATE V

Decay curve for the line at 3805.3 Å. τ_1 is the lifetime in nsec of the upper level of the line. τ_2 is a long-lived component attributed to unresolved low-intensity lines.

PLATE V

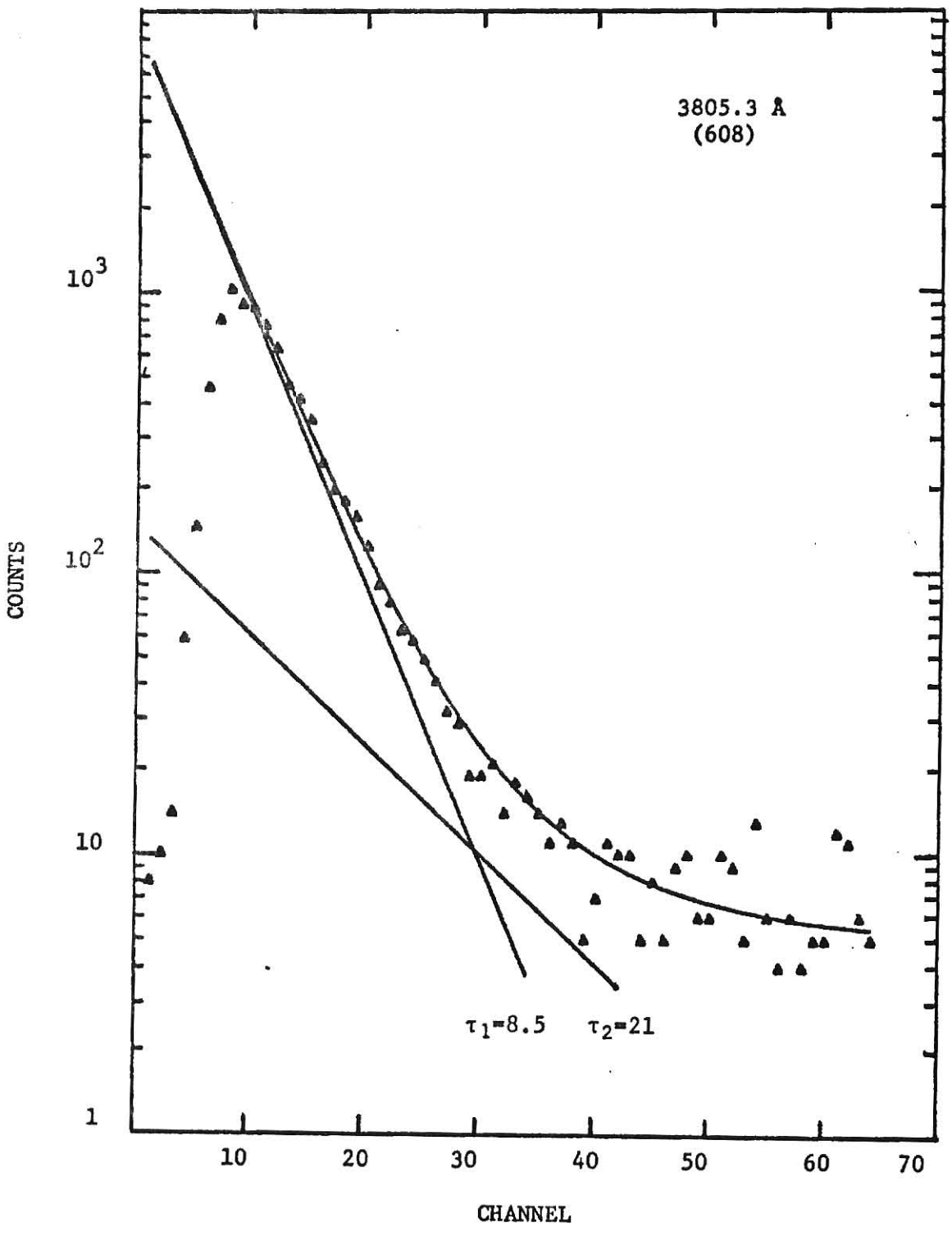
3805.3 Å
(608)
10^3
10^2
10
1
COUNTS
τ_1=8.5
τ_2=21
10
20
30
40
50
60
70
CHANNEL

EXPLANATION OF PLATE VI

Decay curve for the line at 4045.8 Å. τ_1 is the lifetime in nsec of the upper level of the line. τ_2 is a long-lived component attributed to cascading from higher levels into the upper level of the line.

PLATE VI

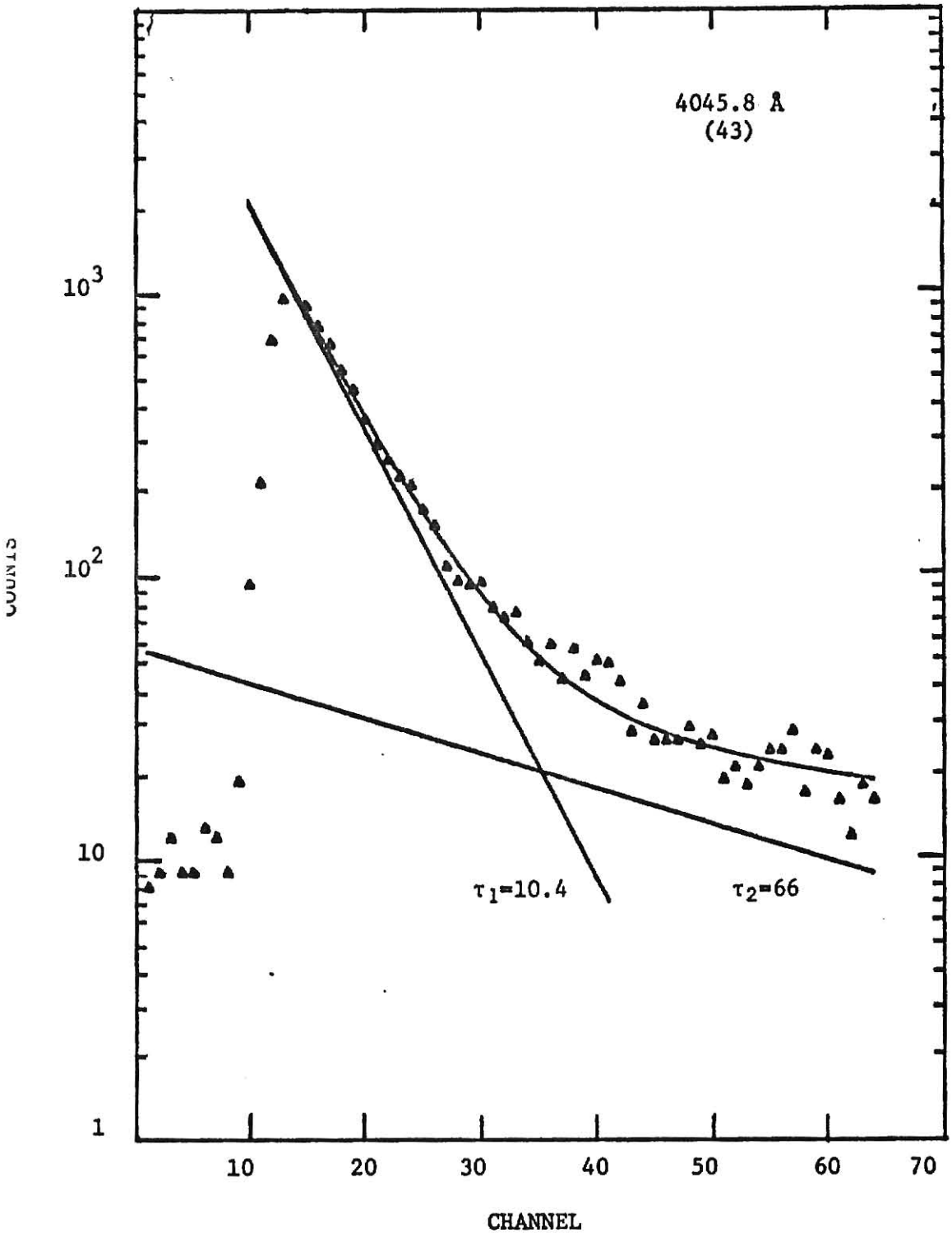
4045.8 Å
(43)
10^3
10^2
10
1
COUNTS
τ_1=10.4
τ_2=66
10
20
30
40
50
60
70
CHANNEL

EXPLANATION OF PLATE VII

Decay curve for the line at 4063.6 Å. τ_1 is the lifetime in nsec of the upper level of the line. τ_2 is a long-lived component attributed to cascading from higher levels into the upper level of the line.

PLATE VII

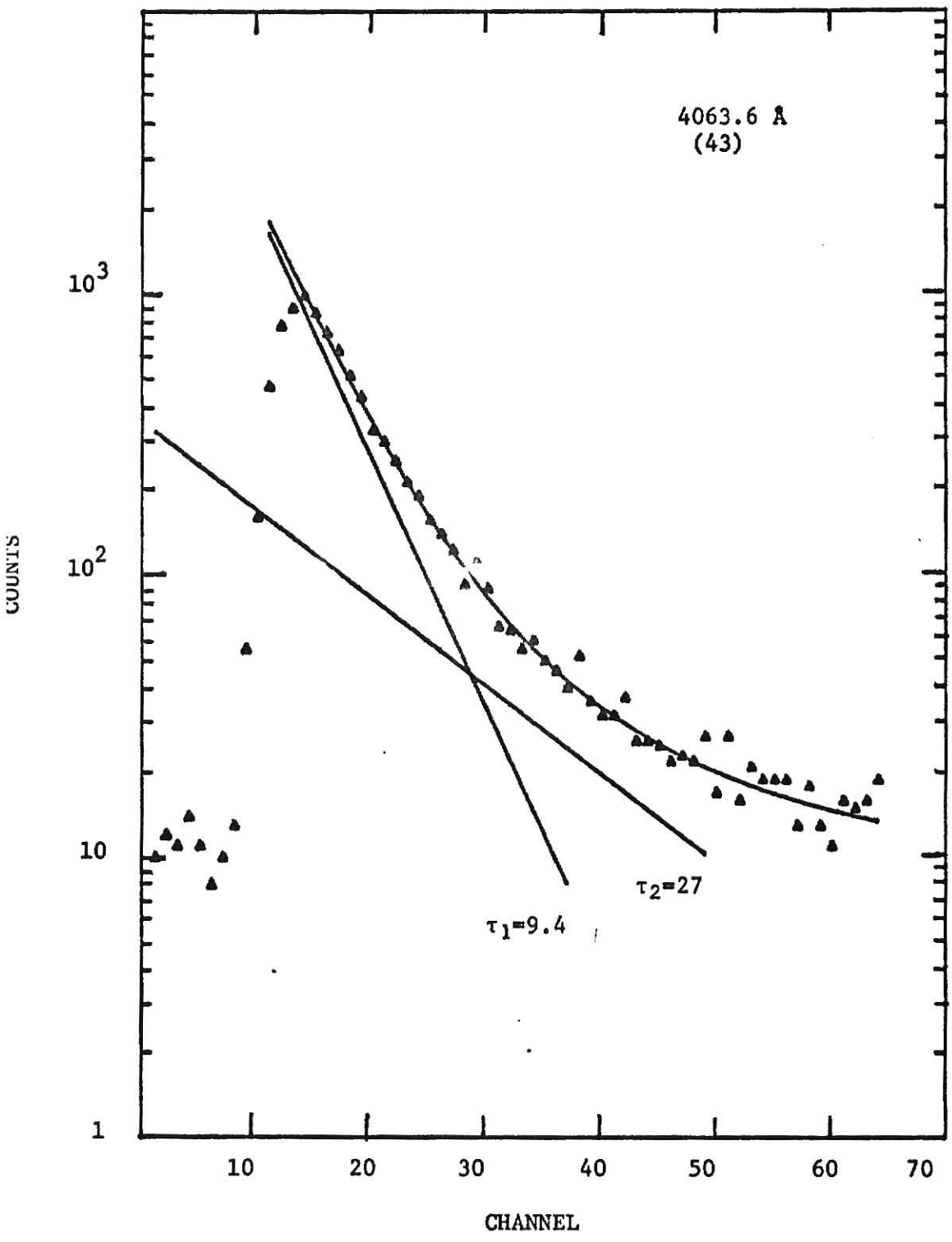
4063.6 Å
(43)
10^3
10^2
10
1
COUNTS
τ_2=27
τ_1=9.4
10
20
30
40
50
60
70
CHANNEL

EXPLANATION OF PLATE VIII

Decay curve for the line at 4071.7 Å. τ_1 is the lifetime in nsec of the upper level of the line. τ_2 is a long-lived component attributed to cascading from higher levels into the upper level of the line.

PLATE VIII

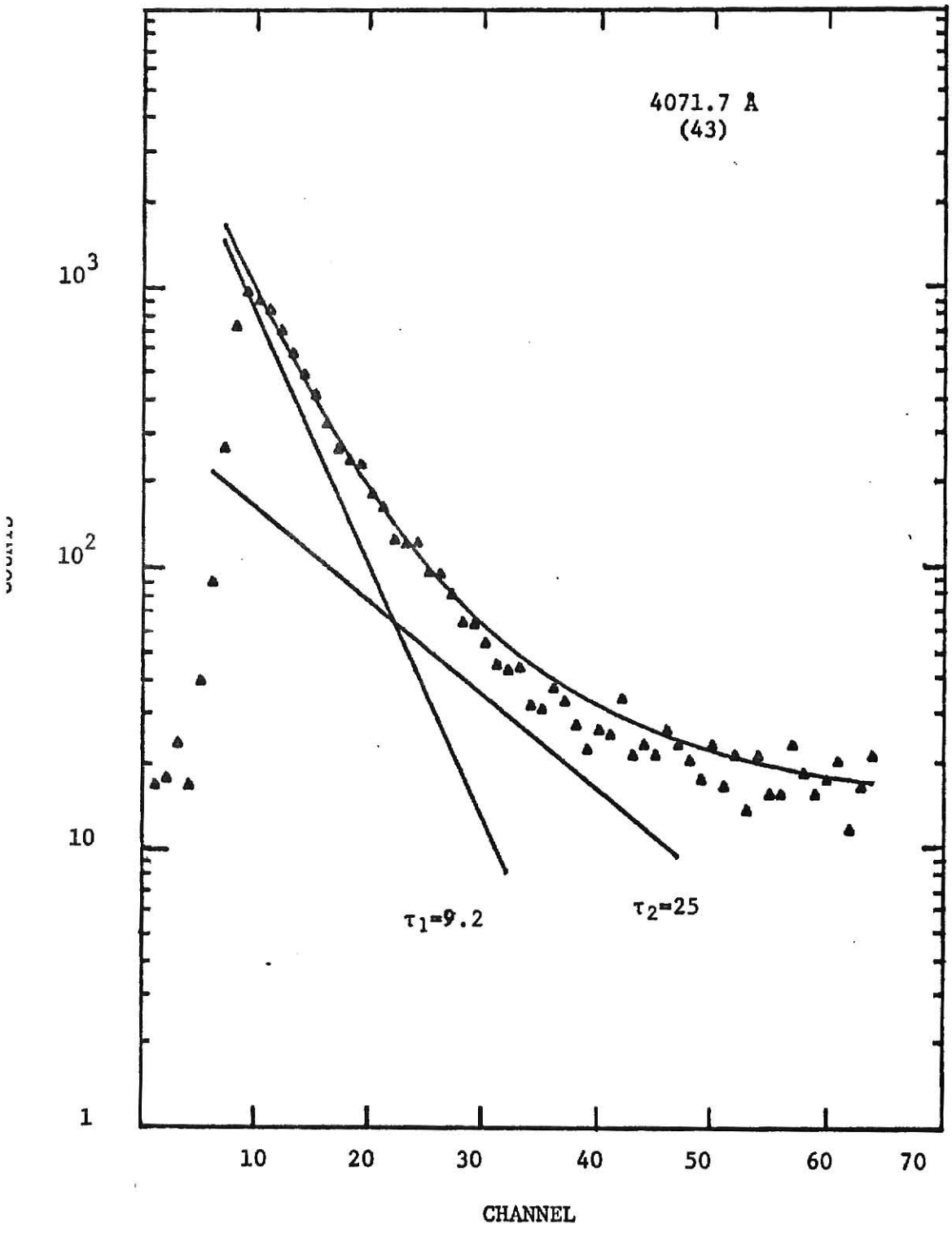
4071.7 Å
(43)
10^3
10^2
10
1
τ_1=9.2
τ_2=25
10
20
30
40
50
60
70
CHANNEL

EXPLANATION OF PLATE IX

Decay curve for the line at 4118.5 Å. τ_1 is the lifetime in nsec of the upper level of the line. τ_2 is a long-lived component attributed to unresolved low-intensity lines.

PLATE IX

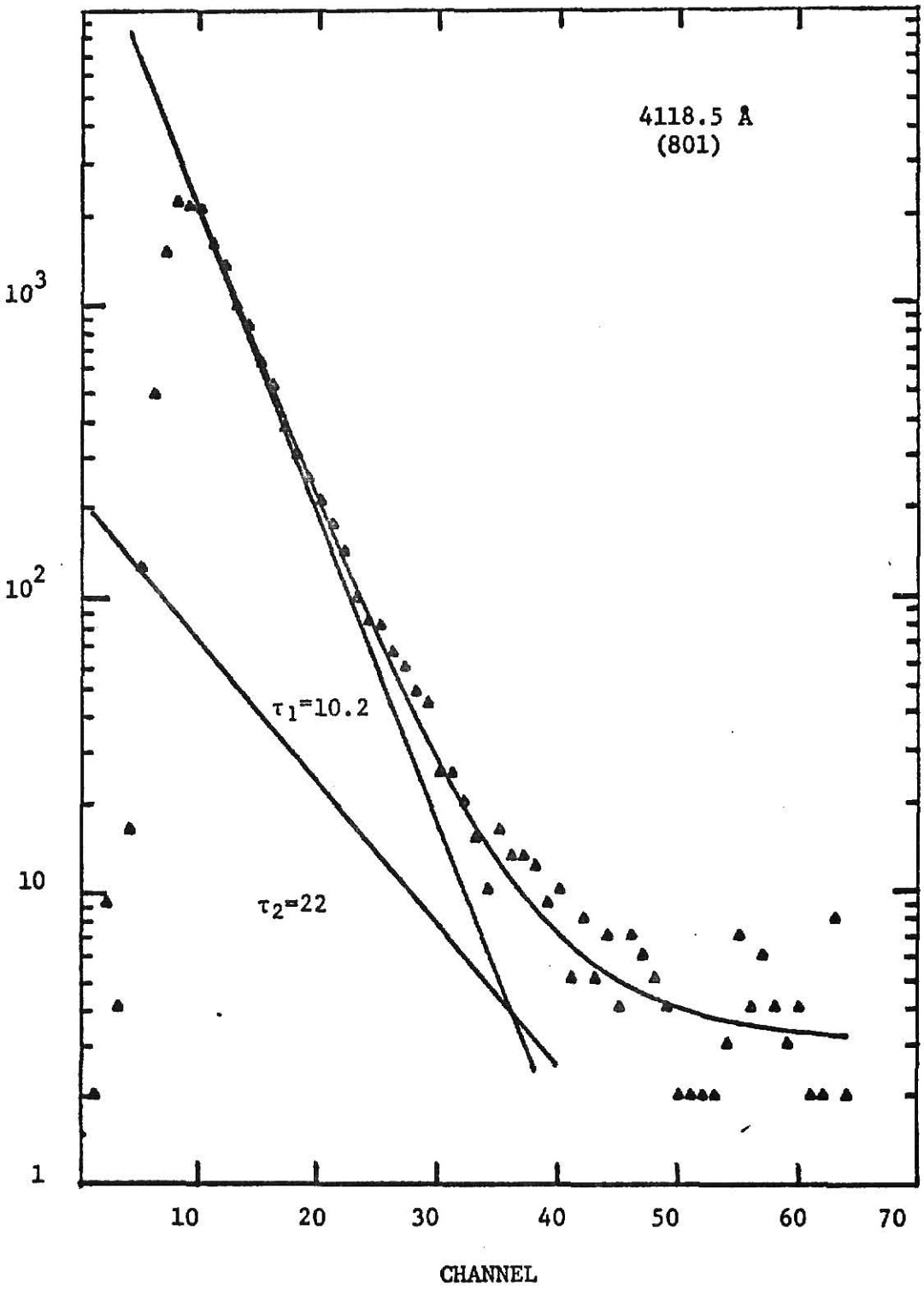
4118.5 Å
(801)
10^3
10^2
10
1
τ_1=10.2
τ_2=22
10
20
30
40
50
60
70
CHANNEL

EXPLANATION OF PLATE X

Decay curve for the line at 4143.4 Å. The lifetimes are not given on this curve because it was impossible to interpret this with any degree of certainty. The curve shows one strong very short-lived component with another strong component having a longer lifetime. Further, this line could not be identified unambiguously because of the presence of two lines with large gA values.

PLATE X

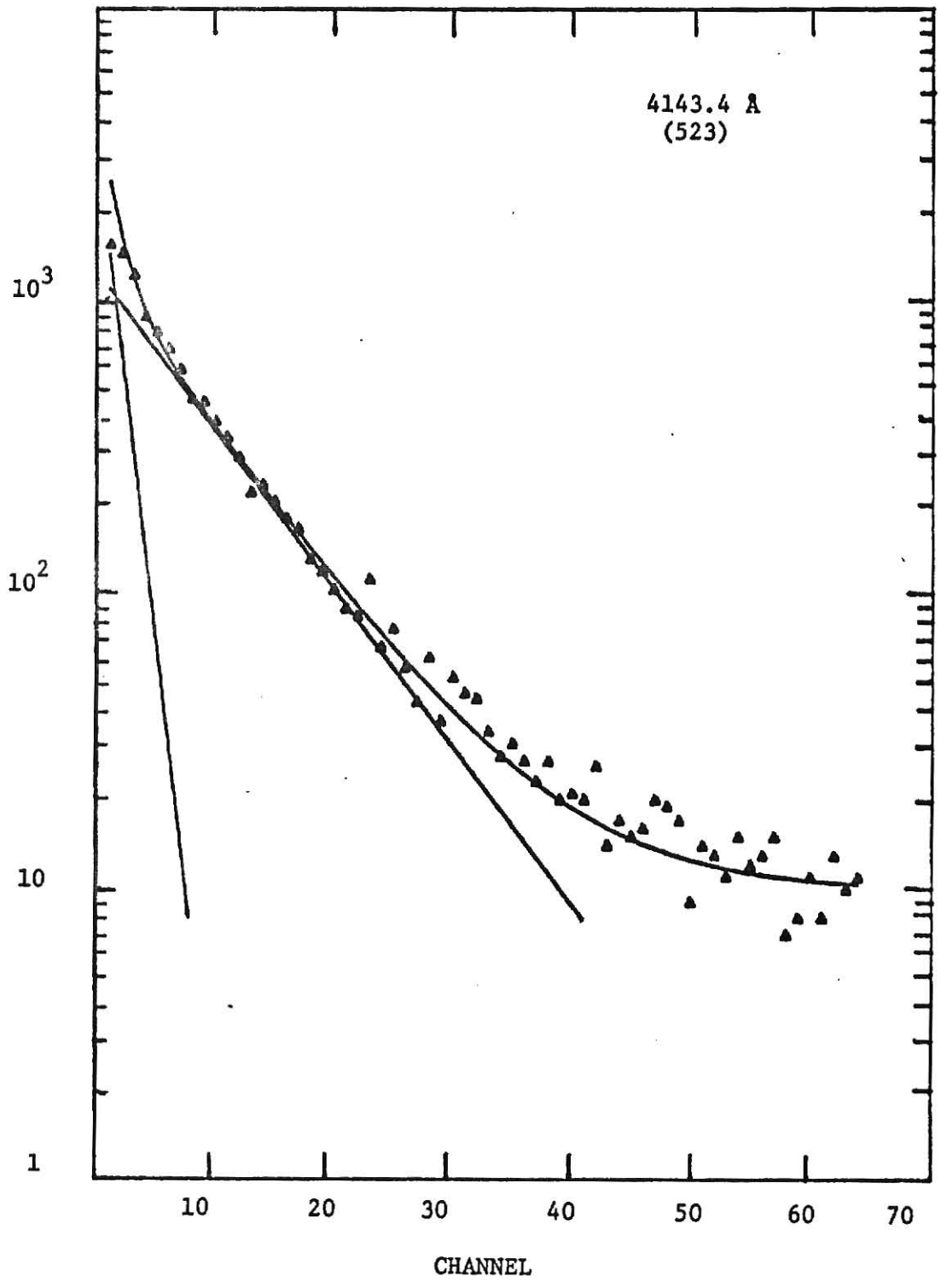

EXPLANATION OF PLATE XI

Decay curve for the line at 4199.1 Å. τ_1 is the lifetime in nsec of the upper level of the line. τ_2 is a long-lived component attributed to unresolved low-intensity lines.

PLATE XI

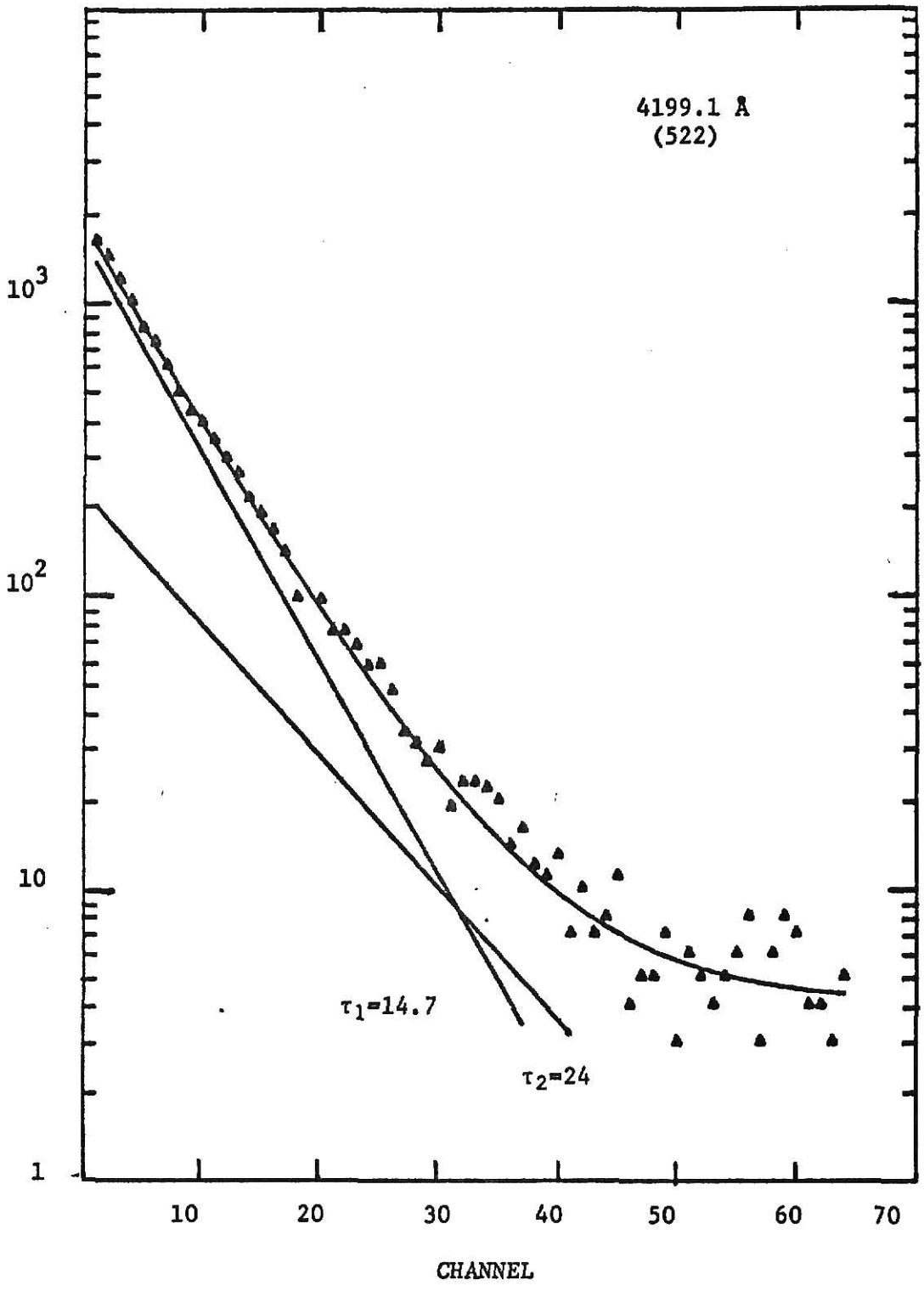
4199.1 Å
(522)
10^3
10^2
10
1
τ_1=14.7
τ_2=24
10
20
30
40
50
60
70
CHANNEL

EXPLANATION OF PLATE XII

Decay curve for the line at 4219.4 Å. τ_1 is the lifetime in nsec of the upper level of the line. τ_2 is a long-lived component attributed to unresolved low-intensity lines.

PLATE XII

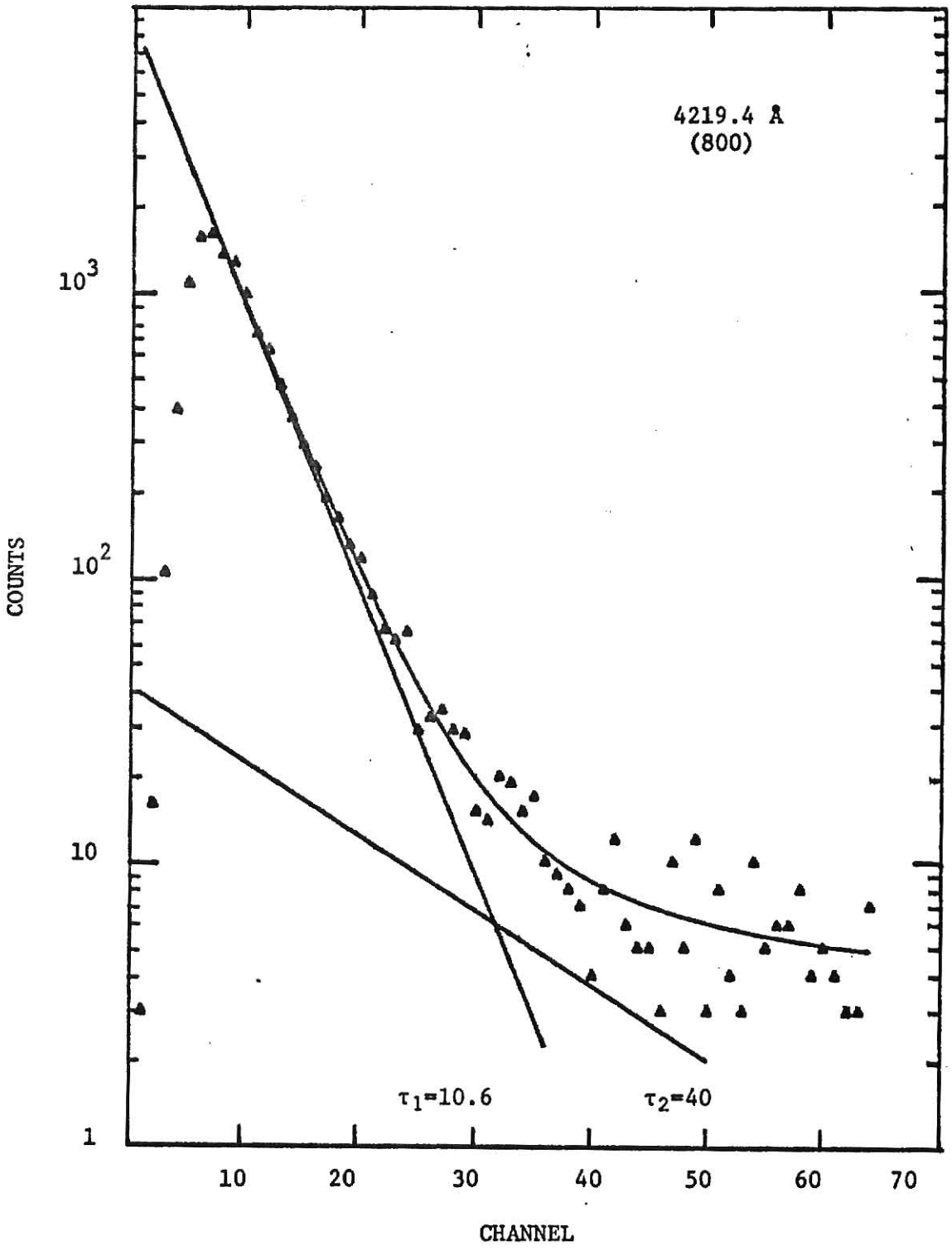
4219.4 Å
(800)
10^3
10^2
10
1
COUNTS
τ_1=10.6
τ_2=40
10
20
30
40
50
60
70
CHANNEL

EXPLANATION OF PLATE XIII

Decay curve for the line at 4271.8 Å. τ_1 is the lifetime in nsec of the upper level of the line. τ_2 is a long-lived component attributed to cascading from higher levels into the upper level of the line.

PLATE XIII

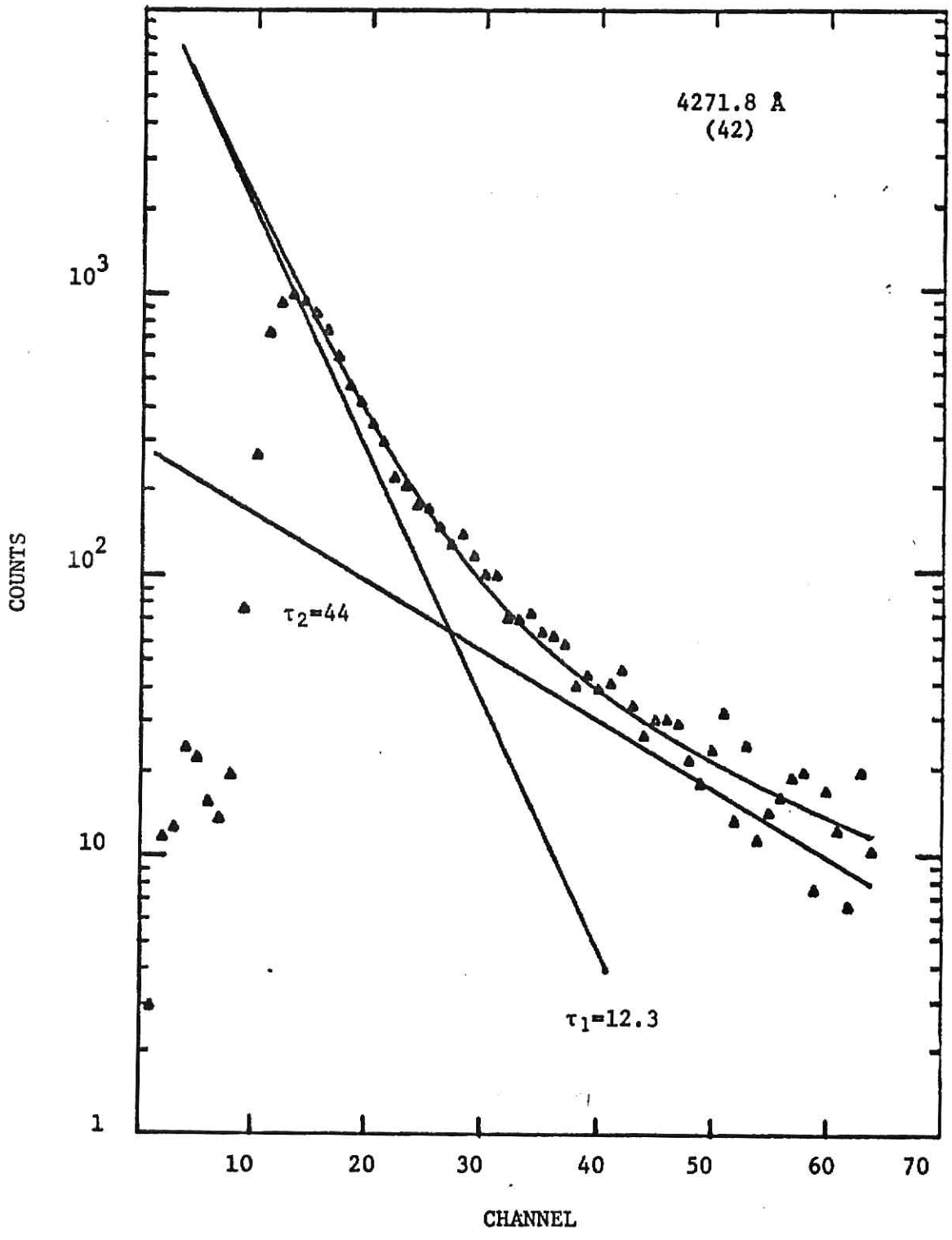
4271.8 Å
(42)
10^3
10^2
10
1
COUNTS
τ_2=44
τ_1=12.3
10
20
30
40
50
60
70
CHANNEL

EXPLANATION OF PLATE XIV

Decay curve for the line at 4307.9 Å. τ_1 is the lifetime in nsec of the upper level of the line. τ_2 is a long-lived component attributed to cascading from higher levels into the upper level of the line.

PLATE XIV

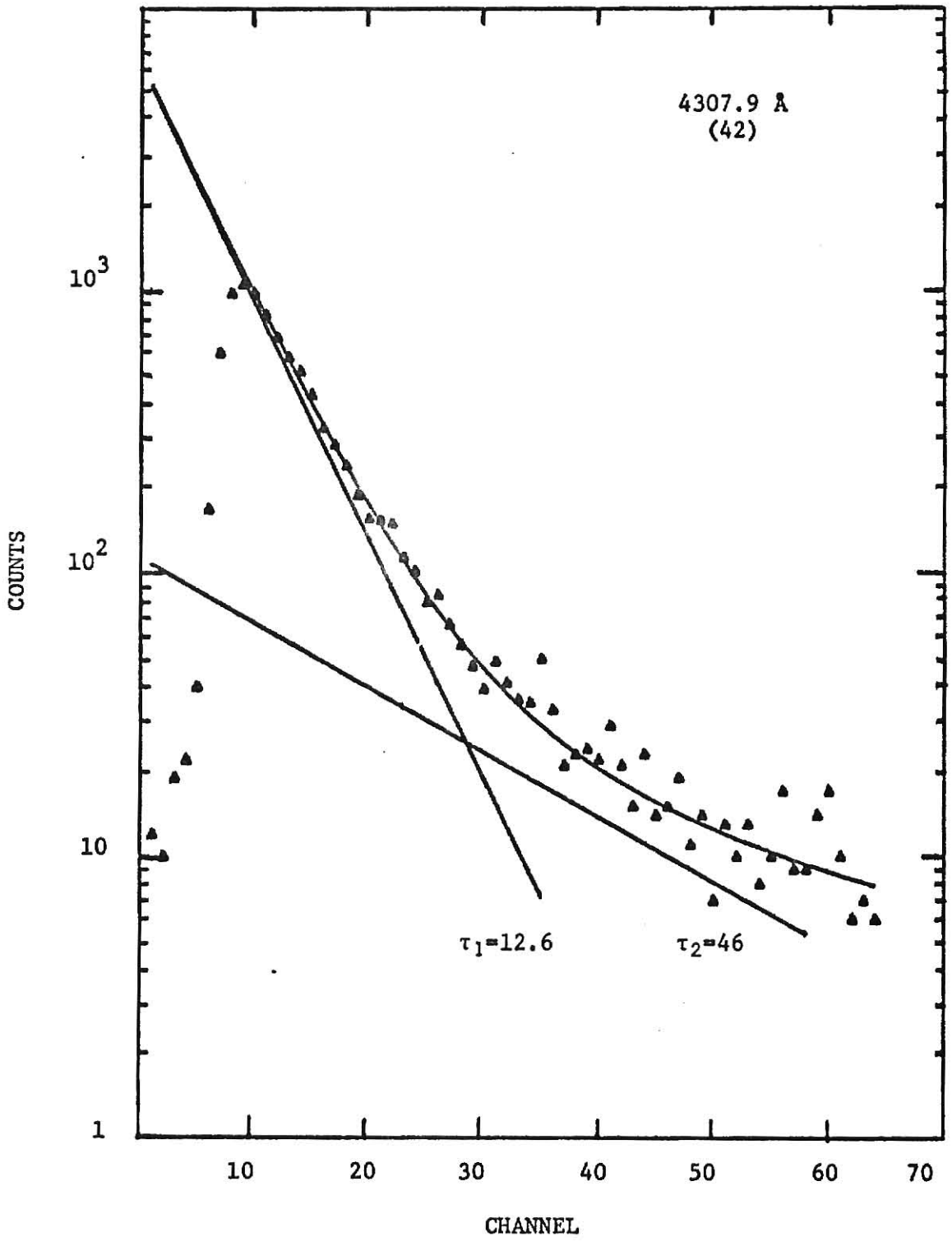
4307.9 Å
(42)
10^3
10^2
10
1
COUNTS
τ_1=12.6
τ_2=46
10
20
30
40
50
60
70
CHANNEL

EXPLANATION OF TABLE IV

Comparison of results. τ_{exp} is the lifetime of the upper level measured in this experiment. The experimental result is compared with the results of several other experiments: Whaling, et.al. 1970 (W); Huber and Parkinson 1971 (HP); Corliss and Bozman 1962 (CB); Bridges and Wiese 1970 (BW). Δlog gf is defined as log gf_{CT} - log gf_{other}. Cascade indicates that this line is fed by cascading lines. There is an identification problem for the line at 3805.3 Å, as indicated in the text.

TABLE IV

Wavelength (Mult.)	Upper Level	τ_{exp}	$\frac{\tau_{exp}}{\tau_W}$	$\frac{\tau_{exp}}{\tau_{CB}}$	Δlog gf HP	Δlog gf CB	Δlog gf BW	log τ_{exp} - log τ_{CT}	Comments
4271.8 (42)	35379	12.3±3.5		6.2	0.18	0.04		0.36	Cascade
4307.9 (42)	35768	12.6±3.5		5.4	0.23	0.10		0.41	Cascade
4045.8 (43)	36686	10.4±3.0		7.1	0.23	-0.06		0.43	Cascade
4063.6 (43)	37163	9.4±3.0		5.5	0.17	0.05		0.40	Cascade
4071.7 (43)	37521	9.2±3.0		6.0	0.25	0.06		0.41	Cascade
4199.1 (522)	48383	14.7±2.0	1.1	7.4	0.48	0.02	0.66	0.68	
4219.4 (800)	52514	10.6±2.0	1.3	9.2		0.15	0.96	0.93	
3765.5 (608)	52655	9.2±1.5	0.95	6.5	0.78	0.29	0.86	0.80	
3805.3 (608)	52899	8.5±1.5		7.7	0.62	0.22		0.85	Identification
4118.6 (801)	53094	10.2±1.5	1.1	10.0	0.59	0.24		0.98	

EXPLANATION OF PLATE IV

Comparison of results. This Plate is a graph of Δlog gf plotted against the excitation potential of the upper levels of the lines. Δlog gf is defined as log gf_{CT} - log gf_{other}. The triangles are the results of this experiment.

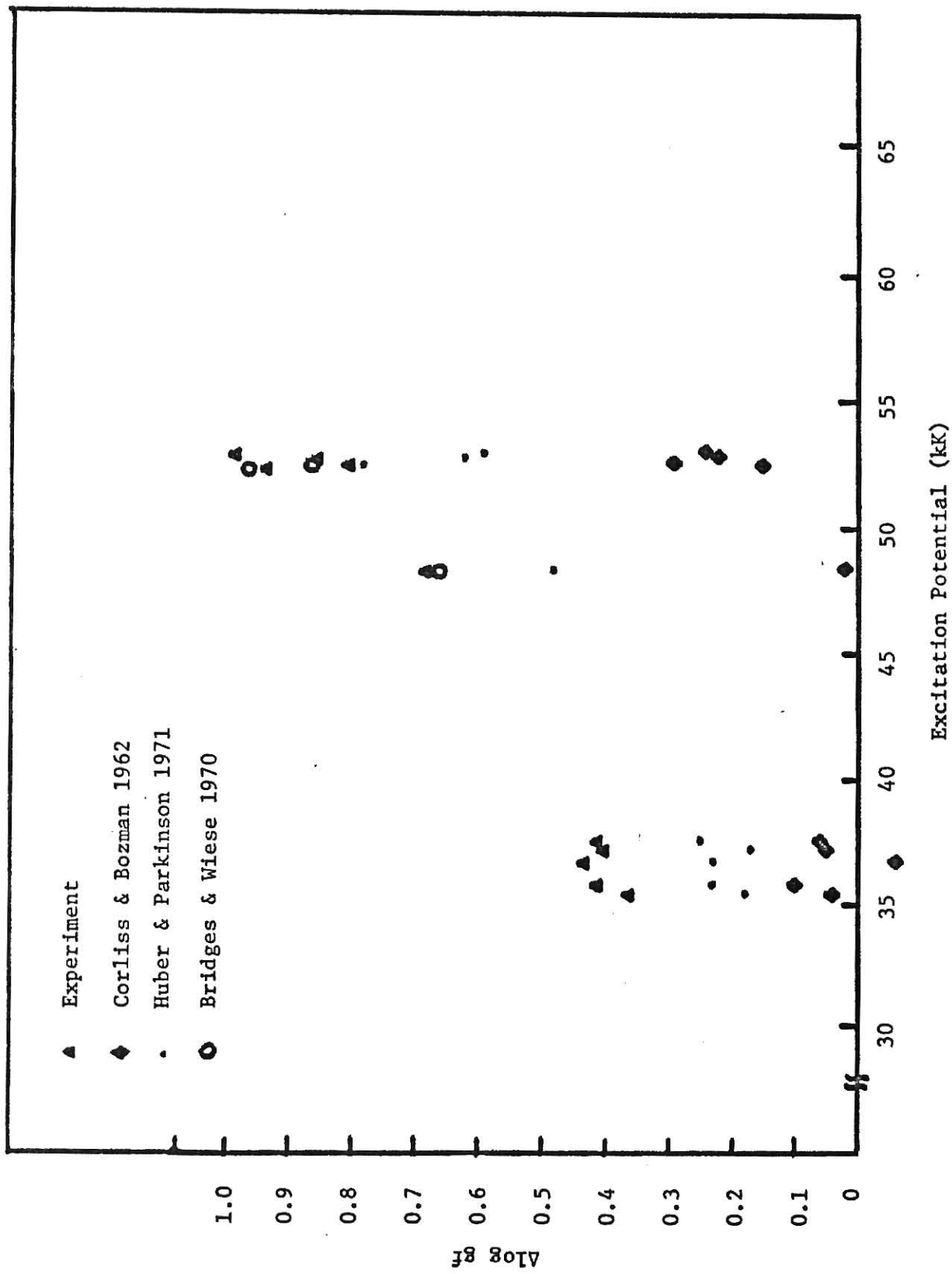
Experiment
Corliss & Bozman 1962
Huber & Parkinson 1971
Bridges & Wiese 1970
Alog gf
1.0
0.9
0.8
0.7
0.6
0.5
0.4
0.3
0.2
0.1
0
30
35
40
45
50
55
60
65
Excitation Potential (kK)

BEAM-FOIL LIFETIMES OF FeI

by

Michael H. Fox

B.S., McPherson College, 1968

AN ABSTRACT OF A MASTER'S THESIS

submitted in partial fulfillment of the

requirements for the degree

MASTER OF SCIENCE

Department of Physics

KANSAS STATE UNIVERSITY

Manhattan, Kansas

1972

ABSTRACT

This paper discusses the use of beam-foil spectroscopy to analyze the spectrum of neutral iron (FeI) and find the mean lifetimes of the upper levels of 10 lines. It further discusses the theory of atomic transition probabilities and evaluates the usefulness of beam-foil spectroscopy in finding absolute transition probabilities.

The lifetimes measured in this experiment are compared with the results of various experiments which have been carried out using beam-foil, arc emission, and shock tube methods. The comparison with the results of Corliss and Tech indicates a variation in their measurements of transition probabilities that depends on the excitation energy of the upper level.